

1 Transcripts with high distal heritability mediate genetic effects on  
2 complex traits

3

4 Anna L Tyler, J Matthew Mahoney, Mark P Keller, Candice N. Baker, Anuj Srivastava, Isabela Gerdes  
5 Gyuricza, [Other Churchill people? Jeff Harder?], Nadia A Rosenthal, Alan D Attie, Gary A Churchill and  
6 Gregory W Carter

7 **Abstract**

8 The effects of genetic variants on complex traits are mediated in large part through regulation of gene  
9 expression. However there has been limited success in explaining variant-trait associations with regulation  
10 of locally encoded genes. There is emerging evidence that distal gene regulation may play an important  
11 role in mediating the effect of genotype on phenotype. Here we investigated the roles of local and distal  
12 gene regulation on complex traits in a mouse model of diet-induced obesity and metabolic disease. We  
13 measured longitudinal metabolic phenotypes in a population of 500 diversity outbred (DO) mice along with  
14 transcriptome-wide gene expression in four disease-relevant tissues: adipose, pancreatic islets, liver, and  
15 skeletal muscle. We developed a novel high-dimensional mediation analysis (HDMA) to model emergent  
16 transcriptomic states mediating genetic effects on traits. We identified a set of tissue-specific composite  
17 transcriptomic signatures that were heritable and trait-related. These transcriptomic signatures were highly  
18 interpretable in terms of biological processes as well as cell type composition in islets and adipose tissue.  
19 The transcripts that contributed most strongly to the composite transcriptomic signatures had low local  
20 heritability and high distal heritability and predicted obesity in an independent population of mice and in  
21 human study populations with high accuracy. In contrast, local expression quantitative trait loci (eQTL)  
22 alone were unable to predict obesity in an independent population. Together these results suggest that  
23 both the tissue used for gene expression analysis as well as distal gene regulation are critically important in  
24 identifying transcriptional mediators of the genome on complex traits.

25 **Introduction**

26 In the quest to understand the genetic architecture of complex traits, gene expression is an important mediator  
27 between genotype and phenotype. There is ample evidence from genome-wide association studies (GWAS)  
28 that regulation of gene expression accounts for the bulk of the genetic effect on complex traits, as most  
29 trait-associated variants lie in gene regulatory regions<sup>1–7</sup>. It is widely assumed that these variants influence  
30 local transcription, and methods such as transcriptome-wide association studies (TWAS)<sup>8–11</sup>, summary  
31 data-based Mendelian randomization (SMR)<sup>10</sup>, and others capitalize on this idea to identify genes associated  
32 with multiple disease traits<sup>12–15</sup>

33 Despite the great promise of these methods, explaining trait effects with local gene regulation has been more  
34 difficult than initially assumed<sup>16;17</sup>. Although trait-associated variants tend to lie in non-coding, regulatory  
35 regions, they often do not have detectable effects on gene expression<sup>16</sup> and tend not to co-localize with  
36 expression quantitative trait loci (eQTLs)<sup>17;18</sup>.

37 One possible explanation for these observations is that gene expression is not being measured in the appropriate  
38 cell types and thus local eQTLs influencing traits cannot be detected<sup>16</sup>. An alternative explanation that has  
39 been discussed in recent years is that effects of these variants are mediated not through local regulation of  
40 gene expression, but through distal regulation<sup>18–20;15</sup>.

41 In this model, a gene's expression is influenced by many variants throughout the genome through their  
42 cumulative effects on a broader regulatory network. In other words, the heritable component of the  
43 transcriptome is an emergent state arising from the myriad molecular interactions defining and constraining  
44 gene expression.

45 To assess the role of wide-spread distal gene regulation on complex traits, we investigated diet-induced obesity  
46 and metabolic disease as an archetypal example. Diet-induced obesity and metabolic disease are genetically  
47 complex with hundreds of variants mapped through GWAS [REFS]. These variants are known to act through  
48 multiple tissues that interact dynamically with each other [REFS], including adipose tissue, pancreatic  
49 islets, liver, and skeletal muscle. The multi-system etiology of metabolic disease complicates mechanistic  
50 dissection of the genetic architecture, requiring large, dedicated data sets that include high-dimensional,  
51 clinically relevant phenotyping, dense genotyping in a highly recombined population, and transcriptome-wide  
52 measurements of gene expression in multiple tissues. Measuring gene expression in multiple tissues is critical  
53 to adequately assess the extent to which local gene regulation varies across multiple tissues and whether such  
54 variability might account for previous failed attempts to identify trait-relevant local eQTL. Such data sets  
55 are extremely difficult to obtain in human populations, particularly in the large numbers of subjects required

56 for adequate statistical power. Thus, to investigate further the role of local and distal gene regulation on  
57 complex traits, we have generated an appropriate data set in a large population of diversity outbred (DO)  
58 mice<sup>21</sup> in a population model of diet-induced obesity and metabolic disease<sup>12</sup>.

59 The DO mice were derived from eight inbred founder mouse strains, five classical lab strains, and three  
60 strains more recently derived from wild mice<sup>21</sup>. They represent three subspecies of mouse *Mus musculus*  
61 *domesticus*, *Mus musculus musculus*, and *Mus musculus castaneus*, and capture 90% of the known variation  
62 in laboratory mice<sup>22</sup>. They are maintained with a breeding scheme that ensures equal contributions from  
63 each founder across the genome thus rendering almost the whole genome visible to genetic inquiry<sup>21</sup>. We  
64 paired clinically relevant metabolic traits from 500 DO mice [REF], including body weight, plasma levels  
65 of insulin and glucose and plasma lipids, with transcriptome-wide gene expression in four tissues related to  
66 metabolic disease: adipose tissue, pancreatic islets, liver, and skeletal muscle. Taken together, these data  
67 enable a comprehensive view into the genetic architecture of metabolic disease.

## 68 Results

### 69 Genetic variation contributed to wide phenotypic variation

70 Although the environment was consistent across all animals, the genetic diversity present in this population  
71 resulted in widely varying distributions across physiological measurements (Fig. 1). For example, body  
72 weights of adult individuals varied from less than the average adult B6 body weight to several times the body  
73 weight of a B6 adult in both sexes (Males: 18.5 - 69.1g, Females: 16.0 - 54.8g) (Fig. 1A). Fasting blood  
74 glucose (FBG) also varied considerably (Fig. 1B) although few of the animals had FBG levels that would  
75 indicate pre-diabetes (19 animals, 3.8%), or diabetes (7 animals, 1.4%) according to previously developed  
76 cutoffs (pre-diabetes: FBG  $\geq$  250 mg/dL, diabetes: FBG  $\geq$  300, mg/dL)<sup>23</sup>. Males had higher FBG than  
77 females on average (Fig. 1C) as has been observed before suggesting either that males were more susceptible  
78 to metabolic disease on the high-fat diet, or that males and females may require different thresholds for  
79 pre-diabetes and diabetes.

80 Body weight was strongly positively correlated with food consumption (Fig. 1D  $R^2 = 0.51, p < 2.2 \times 10^{-16}$ )  
81 and fasting blood glucose (FBG) (Fig. 1E,  $R^2 = 0.21, p < 2.2 \times 10^{-16}$ ) suggesting a link between behavioral  
82 factors and metabolic disease. However, the heritability of this trait and others (Fig. 1F) indicates that  
83 background genetics contribute substantially to correlates of metabolic disease in this population.

84 The trait correlations (Fig. 1G) shows that most of the metabolic trait pairs were weakly correlated indicating  
85 complex relationships among the measured traits. This low level of redundancy suggests a broad sampling of

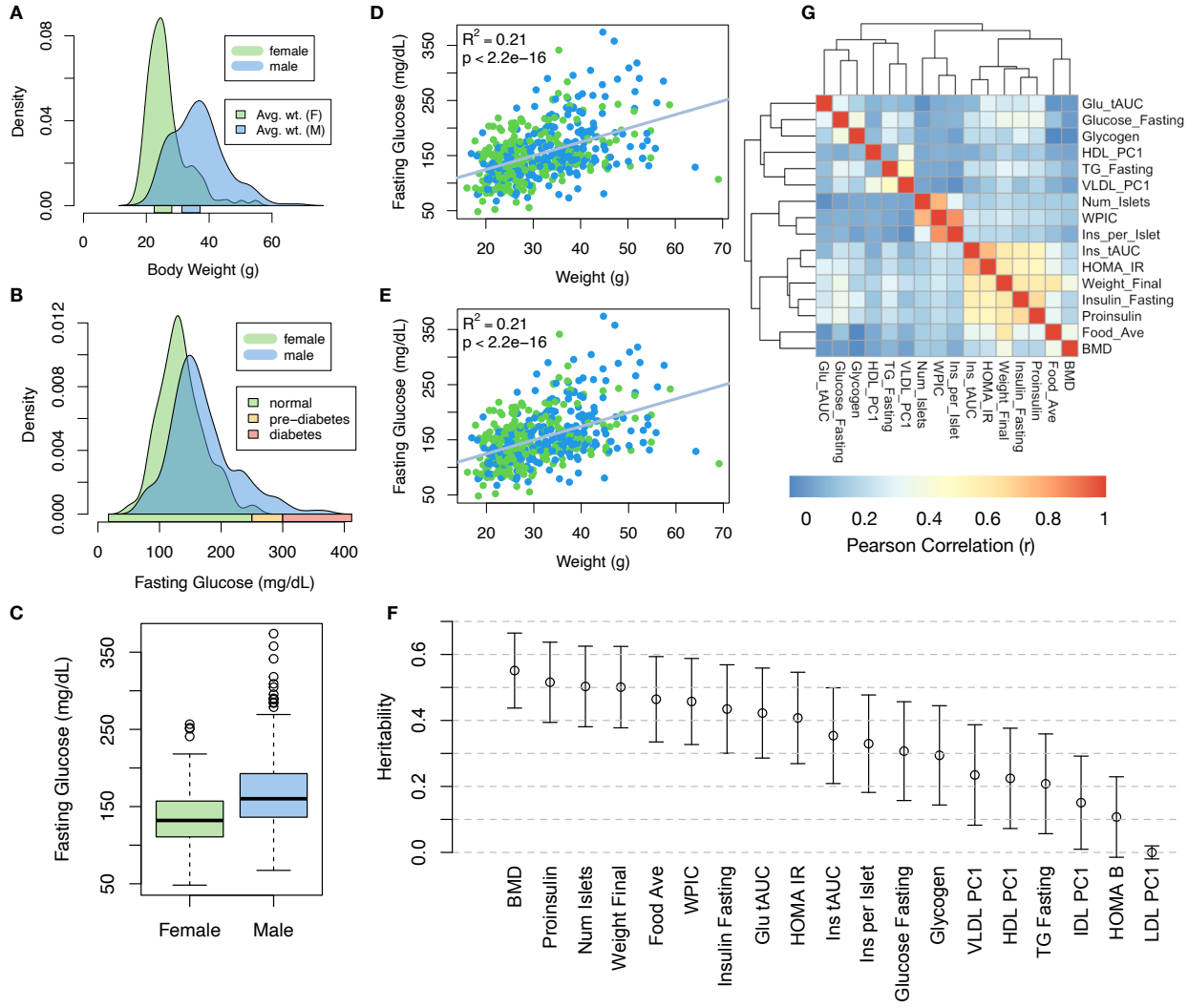


Figure 1: Clinical overview. **A.** Distributions of final body weight in the diversity outbred mice. Sex is indicated by color. The average B6 male and female adult weights at 24 weeks of age are indicated by blue and green bars on the x-axis. **B.** The distribution of final fasting glucose across the population split by sex. Normal, pre-diabetic, and diabetic fasting glucose levels for mice are shown by colored bars along the x-axis. **C.** Males had higher fasting blood glucose on average than females. **D.** The relationship between food consumption and body weight for both sexes. **E.** Relationship between body weight and fasting glucose for both sexes. **F.** Heritability estimates for each physiological trait. Bars show standard error of the estimate. **G.** Correlation structure between pairs of physiological traits.

multiple heritable aspects of metabolic disease including overall body weight, glucose homeostasis, pancreatic composition and liver function.

#### 88 Distal Heritability Correlated with Phenotype Relevance

We performed eQTL analysis using R/qtl2<sup>24</sup> (Methods) and identified both local and distal eQTLs for transcripts in each of the four tissues (Supp. Fig 1). Significant local eQTLs far outnumbered distal eQTLs

91 (Supp. Fig. 1F) and tended to be shared across tissues (Supp. Fig. 1G) whereas the few significant distal  
 92 eQTLs we identified tended to be tissue-specific (Supp. Fig. 1H)

93 We calculated the heritability of each transcript in terms of local and distal genetic factors (Methods). Overall,  
 94 local and distal genetic factors contributed approximately equally to transcript abundance. In all tissues,  
 95 both local and distal factors explained between 8 and 18% of the variance in the median transcript (Fig 2A).

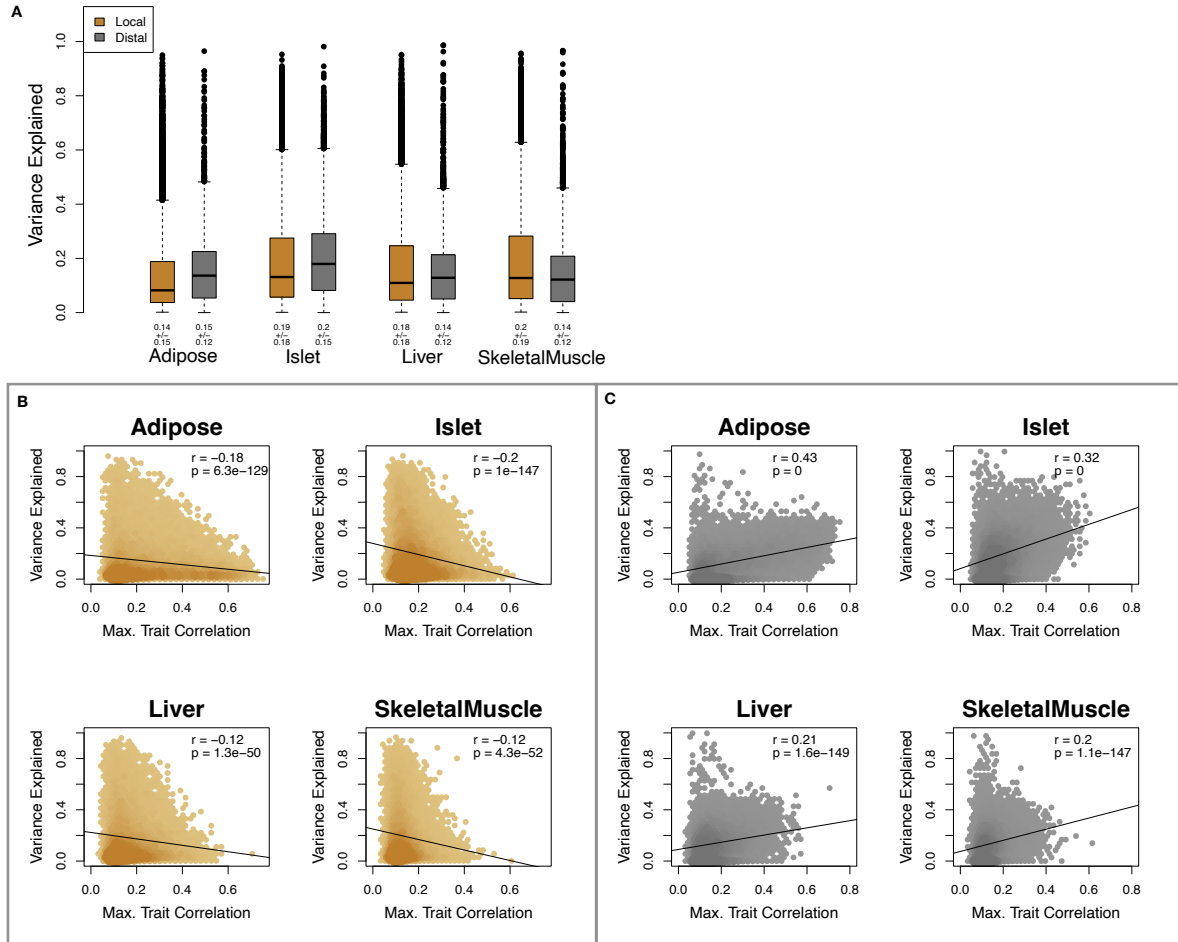


Figure 2: Transcript heritability and trait relevance. **A.** Distributions of distal and local heritability of transcripts across the four tissues. Overall local and distal factors contribute equally to transcript heritability. The relationship between **(B.)** local and **(C.)** distal heritability and trait relevance across all four tissues. Here trait relevance is defined as the maximum correlation between the transcript and all traits. Local heritability was negatively correlated with trait relevance, and distal heritability is positively correlated with trait relevance. Pearson ( $r$ ) and  $p$  values for each correlation are shown in the upper-right of each panel.

96 The local heritability of transcripts was negatively correlated with their trait relevance, defined as the  
 97 maximum correlation of a transcript across all traits (Fig. 2B). This suggests that the more local genotype  
 98 influenced transcript abundance, the less effect this variation had on the measured traits. Conversely, the

99 distal heritability of transcripts was positively correlated with trait relevance (Fig. 2C). That is, transcripts  
100 that were more highly correlated with the measured traits tended to be distally, rather than locally, heritable.  
101 Importantly, this pattern was consistent across all tissues, strongly suggesting that this is a generic finding.  
102 This finding is consistent with previous observations that low-heritability transcripts explain more expression-  
103 mediated disease heritability than high-heritability transcripts<sup>19</sup>. However, the positive relationship between  
104 trait correlation and distal heritability demonstrated further that there are diffuse genetic effects throughout  
105 the genome converging on trait-related transcripts.

106 **High-Dimensional Mediation identified a high-heritability composite trait that was perfectly  
107 mediated by a composite transcript**

108 The above univariate analyses establish the importance of distal heritability for trait-relevant transcripts.  
109 However, the number of transcripts dramatically exceeds the number of degrees of freedom of the phenotype.  
110 Thus, we expect the heritable, trait-relevant transcripts to be highly correlated and organized according  
111 to coherent, emergent biological processes representing the mediating endophenotypes driving clinical trait  
112 variation. To identify these endophenotypes in a theoretically principled way, we developed a novel dimension-  
113 reduction technique, HDMA, that uses the theory of causal graphical models to identify a transcriptomic  
114 signature that is simultaneously 1) highly heritable, 2) strongly correlated to the measured phenotypes, and  
115 3) conforms to the causal mediation hypothesis (Fig. 3). HDMA projects the high-dimensional scores—a  
116 composite genome score ( $G_C$ ), a composite transcriptome score ( $T_C$ ), and a composite phenotype score  
117 ( $P_C$ )—and uses the univariate theory of mediation to constrain these projections to satisfy the hypotheses of  
118 perfect mediation. Specifically, perfect mediation implies that upon controlling for the transcriptomic score,  
119 the genome score is uncorrelated to the phenotype score, which can also be viewed as a constraint on the  
120 correlation coefficients

$$\text{Corr}(G_C, P_C) = \text{Corr}(G_C, T_C)\text{Corr}(T_C, P_C),$$

121 which corresponds to the path coefficient in the mediation model [REF]. Operationally, HDMA is closely  
122 related to generalized canonical correlation analysis, for which provably convergent algorithms have recently  
123 been developed<sup>25</sup>. Implementation details for HDMA are available in **Supp. Methods XXX**.  
124 We used high-dimensioal mediation to identify the major axis of variation in the transcriptome that mediated  
125 the effects of the genome on metabolic traits (Fig 3). Fig. 3A shows the partial correlations ( $\rho$ ) between  
126 the pairs of these composite vectors. The partial correlation between  $G_C$  and  $T_C$  was 0.42, and the partial

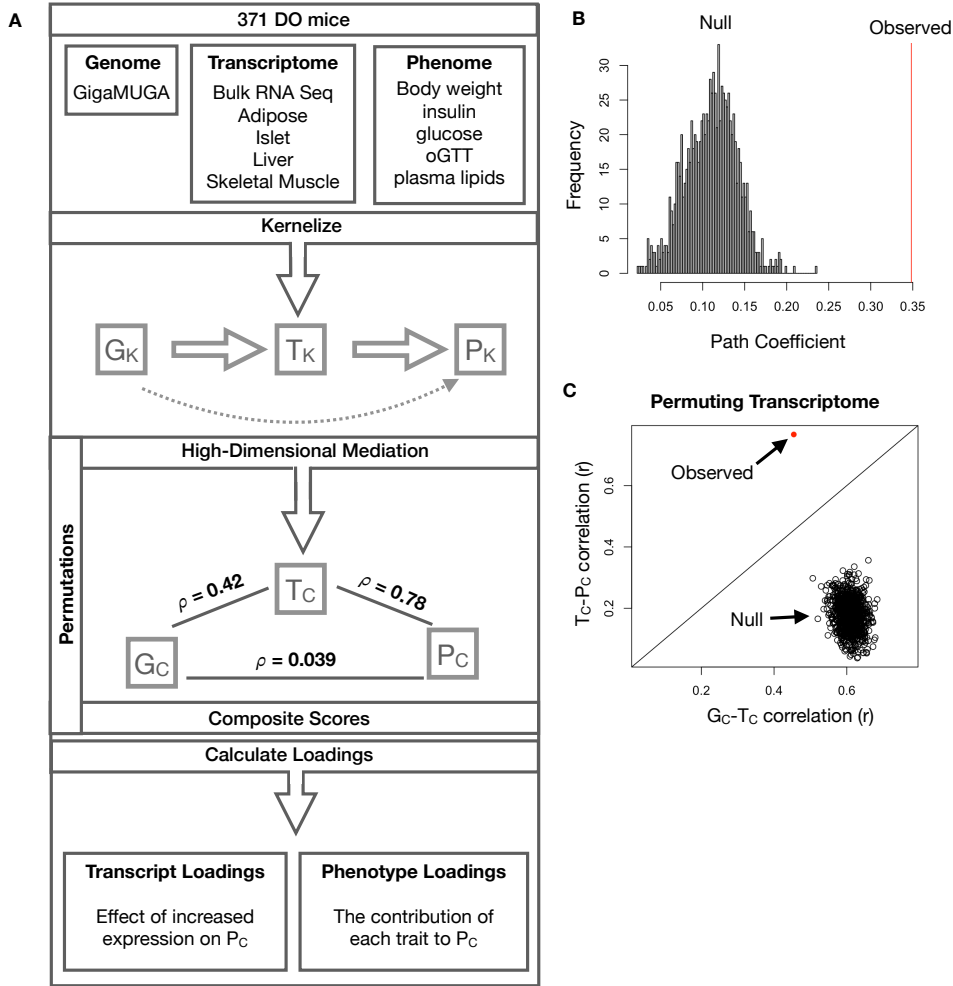


Figure 3: High-dimensional mediation. **A.** Workflow indicating major steps of high-dimensional mediation. The genotype, transcriptome, and phenotype matrices were kernelized to yield single matrices representing the relationships between all individuals for each data modality ( $G_K$  = genome kernel,  $T_K$  = transcriptome kernel;  $P_K$  = phenotype kernel). High-dimensional mediation was applied to these matrices to maximize the direct path  $G \rightarrow T \rightarrow P$ , the mediating pathway (arrows), while simultaneously minimizing the direct  $G \rightarrow P$  pathway (dotted line). The composite vectors that resulted from high-dimensional mediation were  $G_c$ ,  $T_c$ , and  $P_c$ . The partial correlations  $\rho$  between these vectors indicated perfect mediation. Transcript and trait loadings were calculated as described in the methods. **B.** The null distribution of the path coefficient derived from 10,000 permutations compared to the observed path coefficient (red line). **C.** The null distribution of the  $G_c$ - $T_c$  correlation vs. the  $T_c$ - $P_c$  correlation compared with the observed value (red dot).

correlation between  $T_c$  and  $P_c$  was 0.78. However, when the transcriptome was taken into account, the partial correlation between  $G_c$  and  $P_c$  was effectively zero (0.039).  $P_c$  captured 30% of the overall trait variance, and its estimated heritability was  $0.71 \pm 0.084$ , which was higher than any of the measured traits (Fig. 1F). Thus, HDMA identified a maximally heritable metabolic composite trait that was perfectly mediated by a highly heritable component of the transcriptome.

Standard CCA is prone to over-fitting because in any two large matrices it can be trivial to identify highly

correlated composite vectors [REF]. To assess whether our implementation of HDMA was similarly prone to over-fitting in a high-dimensional space, we performed permutation testing. We permuted the individual labels on the transcriptome matrix 1000 times and recalculated the path coefficient, which is the partial correlation of  $G_C$  and  $T_C$  multiplied by the partial correlation of  $T_C$  and  $P_C$ . This represents the path from  $G_C$  to  $P_C$  that is mediated through  $T_C$ . The null distribution of the path coefficient is shown in Fig. 3B, and the observed path coefficient from the original data is indicated by the red line. The observed path coefficient was well outside the null distribution generated by permutations ( $p < 10^{-16}$ ). Fig. 3C illustrates this observation in more detail. Although we identified high correlations between  $G_C$  and  $T_C$ , and modest correlations between  $T_C$  and  $P_C$  in the null data (Fig 3C), these two values could not be maximized simultaneously in the null data. In contrast, the red dot shows that in the real data both the  $G_C$ - $T_C$  correlation and the  $T_C$ - $P_C$  correlation could be maximized simultaneously suggesting that the path from genotype to phenotype through transcriptome is highly non-trivial and identifiable in this case. These results suggest that these composite vectors represent genetically determined variation in phenotype that is mediated through genetically determined variation in transcription.

**Body weight and insulin resistance were highly represented in the expression-mediated composite trait**

Each composite score is simply a weighted combination of the measured variables and the magnitude and sign of the weights, called loadings, correspond the relative importance and directionality of each variable in the composite score. The loadings of each measured trait onto  $P_C$  indicate how much each contributed to the composite phenotype. Final body weight contributed the most (Fig. 4), followed by homeostatic insulin resistance (HOMA\_IR) and fasting plasma insulin levels (Insulin\_Fasting). We can thus interpret  $P_C$  as an index of metabolic disease (Fig. 4B). Individuals with high values of  $P_C$  have a higher metabolic index and greater metabolic disease, including higher body weight and higher insulin resistance. We refer to  $P_C$  as the metabolic index going forward. Traits contributing the least to the metabolic index were measures of cholesterol and pancreas composition. Thus, when we interpret the transcriptomic signature identified by HDMA, we are explaining primarily the transcriptional mediation of body weight and insulin resistance, as opposed to cholesterol measurements.

**High-loading transcripts have low local heritability, high distal heritability, and were linked mechanistically to obesity**

We interpreted large loadings onto transcripts as indicating strong mediation of the effect of genetics on metabolic index. Large positive loadings indicate that higher expression was associated with a higher

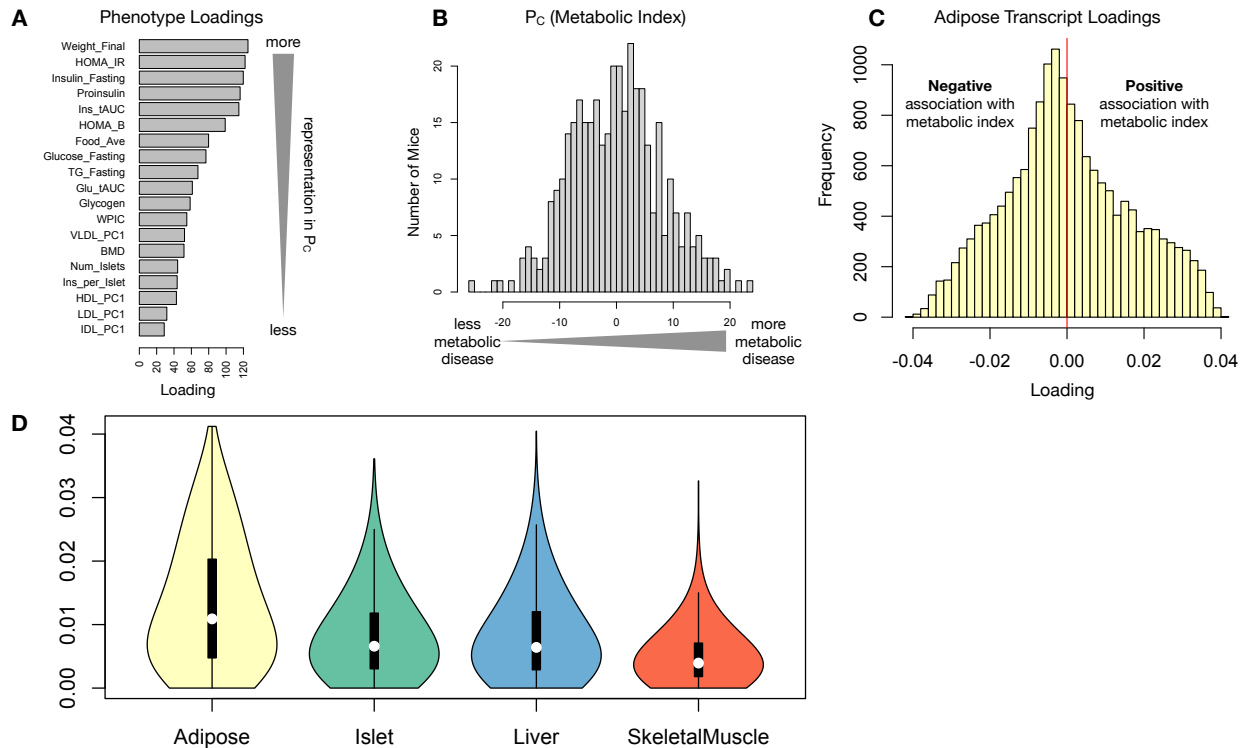


Figure 4: Interpretation of loadings. **A.** Loadings across traits. Body weight and insulin resistance contributed the most to the composite trait. **B.** Phenotype scores across individuals. Individuals with large positive phenotype scores had higher body weight and insulin resistance than average. Individuals with large negative phenotype scores had lower body weight and insulin resistance than average. **C.** Distribution of transcript loadings in adipose tissue. For transcripts with large positive loadings, higher expression was associated with higher phenotype scores. For transcripts with large negative loadings, higher expression was associated with lower phenotype scores. **D.** Distribution of absolute value of transcript loadings across tissues. Transcripts in adipose tissue had the largest loadings indicating that transcripts in adipose tissue were the best mediators of the genetic effects on body weight and insulin resistance.

metabolic index (i.e. higher risk of obesity and metabolic disease on the high-fat diet) (Fig. 4C). Conversely, large negative loadings indicate that high expression of these transcripts was associated with a lower metabolic index (i.e. lower risk of obesity and metabolic disease on the high-fat diet) (Fig. 4C). We used gene set enrichment analysis (GSEA)<sup>26;27</sup> to look for biological processes and pathways that were enriched at the top and bottom of this list (Methods).

In adipose tissue, both GO processes and KEGG pathway enrichments pointed to an axis of inflammation and metabolism (Supp. Fig. 2 and Fig. 11). GO terms and KEGG pathways associated with inflammation, particularly macrophage infiltration, were positively associated with metabolic index, indicating that increased expression in inflammatory pathways was associated with a higher metabolic index. It is well established that adipose tissue in obese individuals is inflamed [cite] and infiltrated by macrophages [cite], and the results here suggest that this may be a heritable component of metabolic disease.

175 The strongest negative enrichments in adipose tissue were related to mitochondrial activity in general, and  
176 thermogenesis in particular (Supp. Fig. 2 and Fig. 11). It has been shown mouse strains with greater  
177 thermogenic potential are also less susceptible to obesity on a high-fat diet [cite].

178 Transcripts associated with the citric acid (TCA) cycle as well as the catabolism of the branched-chain amino  
179 acids (BCAA) (valine, leucine, and isoleucine) were strongly enriched with negative loadings in adipose  
180 tissue (Supp. Fig. 3). Expression of genes in both pathways (for which there is some overlap) has been  
181 previously associated with insulin sensitivity<sup>12;28;29</sup>, suggesting that heritable variation in regulation of these  
182 pathways may influence risk of insulin resistance.

183 Looking at the 10 most positively and negatively loaded transcripts from each tissue, it is apparent that  
184 transcripts in the adipose tissue had the largest loadings, both positive and negative, of all tissues (Fig. 5A  
185 bar plot) This suggests that much of the effect of genetics on body weight and insulin resistance is mediated  
186 through gene expression in adipose tissue. The strongest loadings in liver and pancreas were comparable,  
187 and those in skeletal muscle were the weakest (Fig. 5A), suggesting that less of the genetic effects were  
188 mediated through transcription in skeletal muscle. Heritability analysis showed that transcripts with the  
189 largest loadings had higher distal heritability than local heritability (Fig. 5A heat map and box plot). This  
190 pattern contrasts with transcripts nominated by TWAS (Fig. 5B), which tended to have lower loadings,  
191 higher local heritability and lower distal heritability. Transcripts with the highest local heritability in each  
192 tissue (Fig. 5C) had the lowest loadings.

193 We performed a literature search for the genes in each of these groups along with the terms “diabetes”,  
194 “obesity”, and the name of the expressing tissue to determine whether any of these genes had previous  
195 associations with metabolic disease in the literature (Methods). Multiple genes in each group had been  
196 previously associated with obesity and diabetes (Fig. 5 bolded gene names). Genes with high loadings were  
197 most highly enriched for previous literature support. They were 2.25 more likely than TWAS hits and 3.6  
198 times more likely than genes with high local heritability to be previously associated with obesity or diabetes.

199 **Tissue-specific transcriptional programs were associated with metabolic traits**

200 Clustering of transcripts with top loadings in each tissue showed tissue-specific functional modules associated  
201 with obesity and insulin resistance (Fig. 6A) (Methods). The clustering highlights the importance of immune  
202 activation particularly in adipose tissue. Except for the “mitosis” cluster, which had large positive loadings  
203 in three of the four tissues, all clusters were strongly loaded in only one or two tissues. For example, the lipid  
204 metabolism cluster was loaded most heavily in liver. The positive loadings suggest that high expression of  
205 these genes particularly in the liver was associated with increased metabolic disease. This cluster included

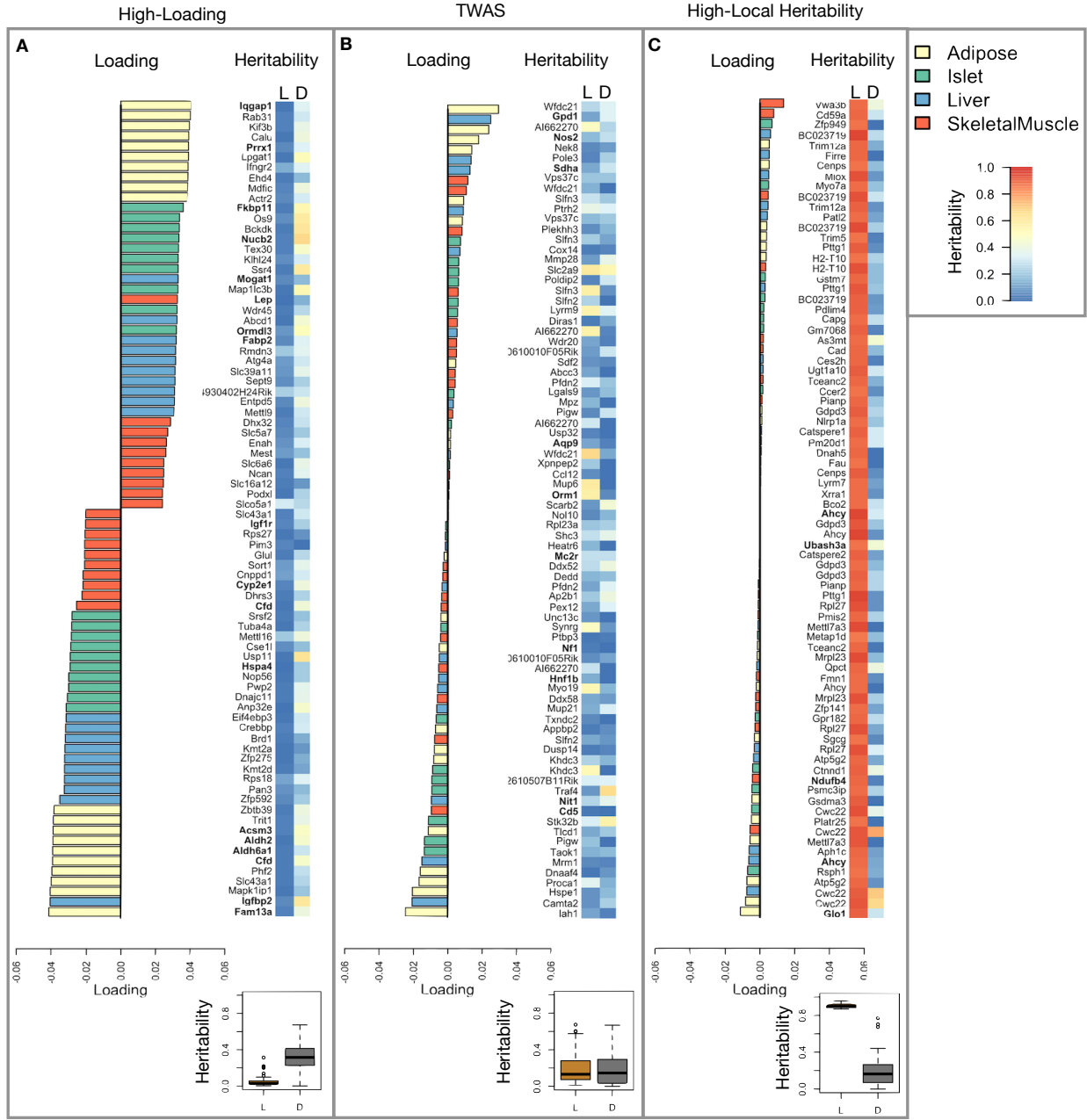


Figure 5: Transcripts with high loadings have high distal heritability and literature support. Each panel has a bar plot showing the loadings of transcripts selected by different criteria. Bar color indicates the tissue of origin. The heat map shows the local (L - left) and distal (D - right) heritability of each transcript. **A.** Loadings for the 10 transcripts with the largest positive loadings and the 10 transcripts with the largest negative loadings for each tissue. **B.** Loadings of TWAS candidates with the 10 largest positive correlations with traits and the largest negative correlations with traits across all four tissues. **C.** The transcripts with the largest local heritability (top 20) across all four tissues.

the gene *Pparg*, whose primary role is in the adipose tissue where it is considered a master regulator of adipogenesis<sup>30</sup>. Agonists of *Pparg*, such as thiazolidinediones, which are FDA-approved to treat type II diabetes, reduce inflammation and adipose hypertrophy<sup>30</sup>. Consistent with this role, the loading for *Pparg*

209 in adipose tissue was negative, suggesting that higher expression was associated with leaner mice (Fig. 6B).  
210 In contrast, *Pparg* had a large positive loading in liver, where it is known to play a role in the development of  
211 hepatic steatosis, or fatty liver. Mice that lack *Pparg* specifically in the liver, are protected from developing  
212 steatosis and show reduced expression of lipogenic genes<sup>31;32</sup>. Overexpression of *Pparg* in the livers of mice  
213 with a *Ppara* knockout, causes upregulation of genes involved in adipogenesis<sup>33</sup>. In the livers of both mice  
214 and humans high *Pparg* expression is associated with hepatocytes that accumulate large lipid droplets and  
215 have gene expression profiles similar to adipocytes<sup>34;35</sup>.

216 The local and distal heritability of *Pparg* is low in adipose tissue suggesting its expression in this tissue is  
217 highly constrained in the population (Fig. 6B). However, the distal heritability of *Pparg* in liver is relatively  
218 high suggesting it is complexly regulated and has sufficient variation in this population to drive variation in  
219 phenotype. Both local and distal heritability of *Pparg* in the islet are relatively high, but the loading is low,  
220 suggesting that variability of expression in the islet does not drive variation in metabolic index. These results  
221 highlight the importance of tissue context when investigating the role of heritable transcript variability in  
222 driving phenotype.

223 Gene lists for all clusters are available in Supplemental File XXX.

#### 224 **Gene expression, but not local eQTLs, predicted body weight in an independent population**

225 To test whether the transcript loadings identified in the DO could be translated to another population, we  
226 tested whether they could predict metabolic phenotype in an independent population of CC-RIX mice, which  
227 were F1 mice derived from multiple pairings of Collaborative Cross (CC) [cite] strains (Fig. 7) (Methods).  
228 We tested two questions. First, we asked whether the loadings identified in the DO mice were relevant to  
229 the relationship between the transcriptome and the phenome in the CC-RIX. We predicted body weight (a  
230 surrogate for metabolic index) in each CC-RIX individual using measured gene expression in each tissue and  
231 the transcript loadings identified in the DO (Methods). The predicted body weight and acutal body weight  
232 were highly correlated in all tissues (Fig. 7B left column). The best prediction was achieved for adipose  
233 tissue, which supports the observation in the DO that adipose expression was the strongest mediator of the  
234 genetic effect on metabolic index. This result also confirms the validity and translatability of the transcript  
235 loadings and their relationship to metabolic disease.

236 The second question related to the source of the relevant variation in gene expression. If local regulation was  
237 the predominant factor influencing gene expression, we should be able to predict phenotype in the CC-RIX  
238 using transcripts imputed from local genotype (Fig. 7A). The DO and the CC-RIX were derived from the  
239 same eight founder strains and so carry the same alleles throughout the genome. We imputed gene expression

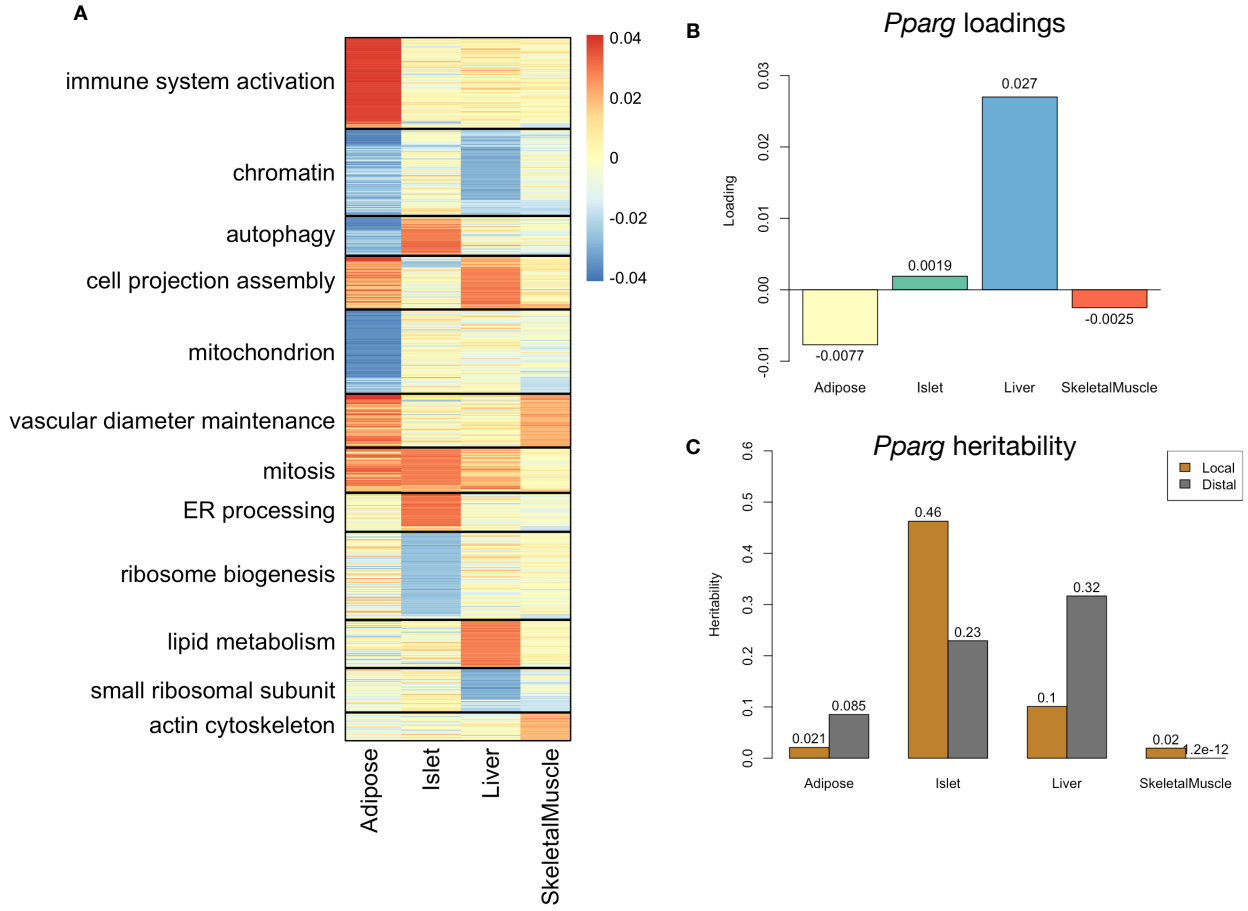


Figure 6: Tissue-specific transcriptional programs were associated with obesity and insulin resistance. **A** Heat map showing the loadings of all transcripts with loadings greater than 2.5 standard deviations from the mean in any tissue. The heat map was clustered using k medoid clustering. Functional enrichments of each cluster are indicated along the left margin. **B** Loadings for *Pparg* in different tissues. **C** Local and distal of *Pparg* expression in different tissues.

240 in the CC-RIX using local genotype and were able to estimate variation in gene transcription robustly (Supp.  
 241 Fig. 4). However, these imputed values failed to predict body weight in the CC-RIX when weighted with the  
 242 loadings from HDMA. (Fig. 7B right column). This result suggests that local regulation of gene expression is  
 243 not the primary factor driving heritability of complex traits, consistent with our findings in the DO population  
 244 that distal heritability was a major driver of trait-relevant variation and that high-loading transcripts had  
 245 comparatively high distal and low local heritability.

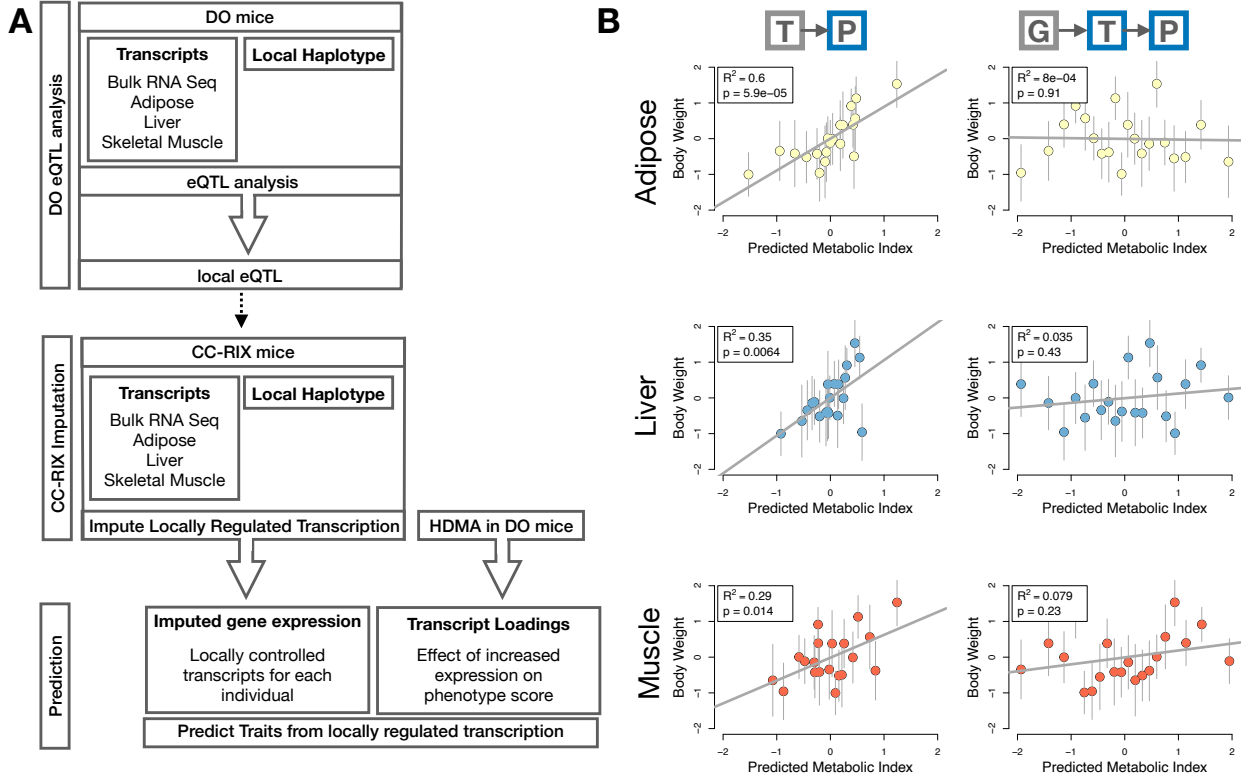


Figure 7: Transcription, but not local genotype, predicts phenotype in the CC-RIX. **A.** Workflow showing procedure for translating HDMA results to an independent population of mice. **B.** Relationships between the predicted metabolic index and measured body weight. The left column shows the predictions using measured transcripts. The right column shows the prediction using transcript levels imputed from local genotype. Gray boxes indicate measured quantities, and blue boxes indicate calculated quantities. The dots in each panel represent individual CC-RIX strains. The gray lines show the standard deviation on body weight for the strain.

246 **Distally heritable transcriptomic signatures reflected variation in composition of adipose tissue  
247 and islets**

248 The interpretation of global genetic influences on gene expression and phenotype is potentially more challenging  
249 than the interpretation and translation of local genetic influences, as genetic effects cannot be localized to  
250 individual gene variants or transcripts. However, there are global patterns across the loadings that can  
251 inform mechanism. For example, heritable variation in cell type composition can be derived from transcript  
252 loadings. We observed above that immune activation in the adipose tissues was an important driver of obesity  
253 in the DO population. To determine whether this is reflected as an increase in macrophages in adipose  
254 tissue, we compared loadings of cell-type specific genes in adipose tissue (Methods). The mean loading  
255 of macrophage-specific genes was significantly greater than 0 (Fig. 8A), indicating that obese mice were  
256 genetically predisposed to have high levels of macrophage infiltration in adipose tissue in response to the  
257 high-fat, high-sugar diet.

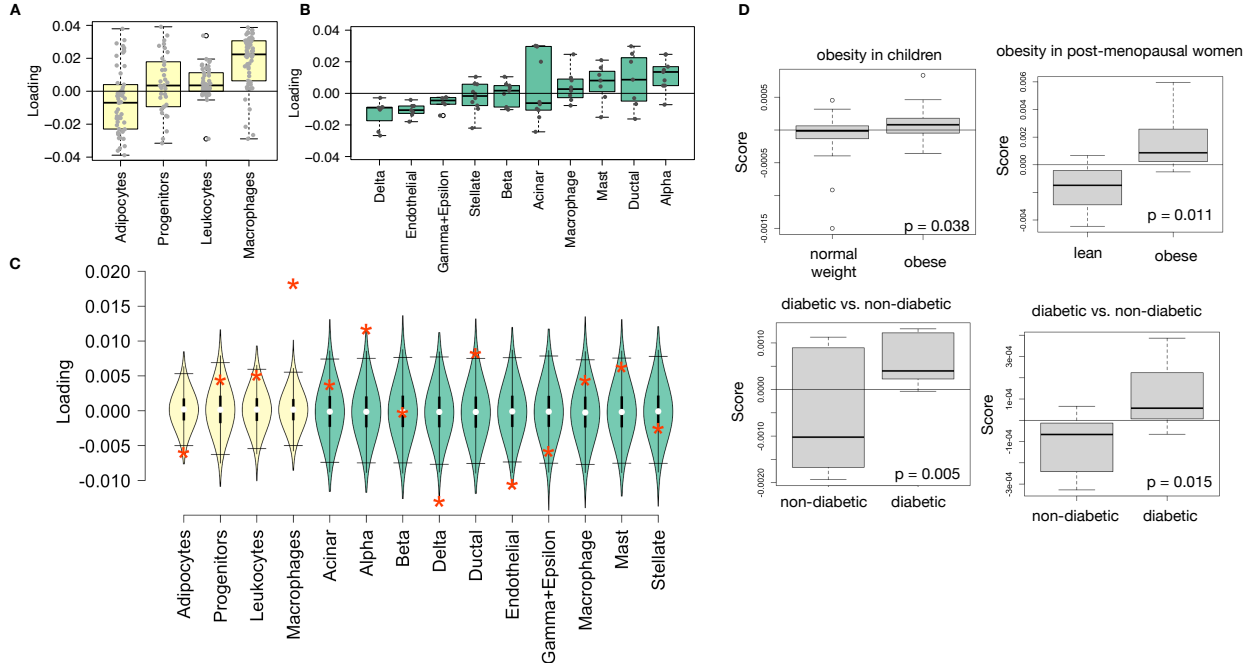


Figure 8: HDMA results translate to humans. **A.** Distribution of loadings for cell-type-specific transcripts in adipose tissue. **B.** Distribution of loadings for cell-type-specific transcripts in pancreatic islets (green). **C.** Null distributions for the mean loading of randomly selected transcripts in each cell type compared with the observed mean loading of each group of transcripts (red asterisk). **D.** Predictions of metabolic phenotypes in four adipose transcription data sets downloaded from GEO. In each study the obese/diabetic patients were predicted to have greater metabolic disease than the lean/non-diabetic patients based on the HDMA results from DO mice.

258 We also compared loadings of cell-type specific transcripts in islet (Methods). The mean loadings for alpha-cell  
 259 specific transcripts were significantly greater than 0, while the mean loadings for delta- and endothelial-cell  
 260 specific genes were significantly less than 0 (Fig. 8B). These results suggest either that mice with higher  
 261 metabolic index had inherited a higher proportions of alpha cells, and lower proportions of endothelial and  
 262 delta cells in their pancreatic islets, that such compositional changes were induced by the HFHS diet in a  
 263 heritable way, or both. In either case, these results support the hypothesis that alterations in islet composition  
 264 drive variation in metabolic index.

265 Notably, the loadings for pancreatic beta cell-type specific loadings was not significantly different from zero.  
 266 This is not necessarily reflective of the function of the beta cells in the obese mice, but rather suggests that  
 267 any variation in the number of beta cells in these mice was unrelated to obesity and insulin resistance. This  
 268 is further consistent with the islet composition traits having small loadings in the phenotype score (Fig. 4).

269 **Heritable transcriptomic signatures translated to human disease**

270 Ultimately, the heritable transcriptomic signatures that we identified in DO mice will be useful if they inform  
271 pathogenicity and treatment of human disease. To investigate the potential for translation of the gene  
272 signatures identified in DO mice, we compared them to transcriptional profiles in obese and non-obese human  
273 subjects (Methods). We limited our analysis to adipose tissue because the adipose tissue signature had the  
274 strongest relationship to obesity and insulin resistance in the DO.

275 We calculated a predicted obesity score for each individual in the human studies based on their adipose  
276 tissue gene expression (Methods) and compared the predicted scores for obese and non-obese groups as well  
277 as diabetic and non-diabetic groups. In all cases, the predicted obesity scores were higher on average for  
278 individuals in the obese and diabetic groups compared with the lean and non-diabetic groups (Fig. 8D).  
279 This indicates that the distally heritable signature of obesity identified in DO mice is relevant to obesity and  
280 diabetes in human subjects.

281 **Targeting gene signatures**

282 Another potential application of the transcript loading landscape is in ranking potential drug candidates  
283 for the treatment of metabolic disease. Although high-loading transcripts may be good candidates for  
284 understanding specific biology related to obesity, the transcriptome overall is highly interconnected and  
285 redundant, and focusing on individual transcripts for treatment may be less effective than using broader  
286 transcriptomic signatures that capture the emergent biology [cite or remove]. The ConnectivityMap (CMAP)  
287 database [cite] developed by the Broad Institute allows us to query thousands of compounds that reverse or  
288 enhance the extreme ends of transcriptomic signatures in multiple different cell types. By identifying drugs  
289 that reverse pathogenic transcriptomic signatures, we can potentially identify compounds that have favorable  
290 effects on gene expression.

291 To test this hypothesis, we queried the CMAP database through the CLUE online query tool [cite] (Methods).  
292 We identified top anti-correlated hits both across all cell types, as well as in adipocytes and pancreatic tumor  
293 cells (Supplemental Figure XXX and XXX).

294 Looking broadly across cell types, the notable top hits from the adipose tissue loadings included mTOR  
295 inhibitors and glucocorticoid agonists (Supplemental Figure XXX). It is thought that metformin, which  
296 is commonly used to improve glycemic control, acts, at least in part, by inhibiting mTOR signaling<sup>36,37</sup>.  
297 However, long-term use of other mTOR inhibitors, such as rapamycin, are known to cause insulin resistance  
298 and  $\beta$ -cell toxicity<sup>37-39</sup>. Glucocorticoids are used to reduce inflammation, which was a prominent signature

299 in the adipose tissues, but these drugs also promote hyperglycemia and diabetes<sup>40;41</sup>. Accute treatment  
300 with glucocorticoids has further been shown to reduce thermogenesis in rodent adipocytes<sup>42–44</sup>, but increase  
301 thermogenesis in human adipocytes<sup>45;46</sup>. Thus, the pathways identified by CMAP across all cell types were  
302 highly related to the transcript loading profiles, but the relationship was not a simple reversal.

303 The top hit in adipocytes was a PARP inhibitor (Supplemental Figure XXXB). PARPs play a role in lipid  
304 metabolism and are involved in the development of obesity and diabetes<sup>47</sup>. PARP1 inhibition increases  
305 mitochondrial biogenesis<sup>48</sup>. Inhibition of PARP1 activity can further prevent necrosis in favor of the less  
306 inflammatory apoptosis<sup>49</sup>, thereby potentially reducing inflammation in stressed adipocytes. Other notable  
307 hits in the top 20 were BTK inhibitors, which have been observed to suppress inflammation and improve  
308 insulin resistance<sup>50</sup> as well as to reduce insulin antibodies in type I diabetes<sup>51</sup>, and IKK inhibitors have been  
309 shown to improve glucose control in type II diabetes<sup>52;53</sup>.

310 The CMAP database includes assays in multiple cell types. Among the top hits for the query with transcript  
311 loadings from pancreatic islets (Fig. XXX), was suppression of T cell receptor signaling, which is known to  
312 be involved in Type 1 diabetes<sup>54</sup>, as well as TNFR1, which has been associated with mortality in diabetes  
313 patients<sup>55</sup>. Suppression of NOD1/2 signaling was also among the top hits. NOD1 and 2 sense ER stress<sup>56;57</sup>,  
314 which is associated with  $\beta$ -cell death in type 1 and type 2 diabetes<sup>58</sup>. This cell death process is dependent  
315 on NOD1/2 signaling<sup>56</sup>, although the specifics have not yet been worked out.

316 Among the top hits in pancreatic tumor cells were known diabetes drugs, including sulfonylureas, PPAR  
317 receptor agonists, and insulin sensitizers. Rosiglitazone is a PPAR- $\gamma$  agonist and was one of the most  
318 prescribed drugs for type 2 diabetes before its use was reduced due to cardiac side-effects<sup>59</sup>. Sulfonylureas  
319 are another commonly prescribed drug class for type 2 diabetes, but also have notable side effects including  
320 hypoglycemia and accellerated  $\beta$ -cell death<sup>60</sup>.

## 321 Discussion

322 Here we used a novel high-dimensional mediation analysis (HDMA) to investigate the relative contributions  
323 of local and distal gene regulation to trait variation in a genetically diverse mouse model of diet-induced  
324 obesity and metabolic disease. It has frequently been assumed that gene regulation in *cis* is the primary  
325 driver of trait variation, but attempts to use local gene regulation to explain phenotypic variation have had  
326 limited success<sup>16;17</sup>. In recent years, the discussion has turned to distal gene regulation<sup>19;18;61</sup>, which is more  
327 complex to identify, but may be an important component of trait heritability.

328 With HDMA we identified tissue-specific composite transcripts that mediated the effects of genetic background

329 on trait variation in the DO mice. The transcripts that contributed the most to the composite transcripts  
330 were strongly distally regulated and only weakly locally regulated, suggesting that distal gene regulation  
331 plays a primary role in driving heritable trait variation. In support of this hypothesis, we demonstrated that  
332 the transcriptomic signatures we identified predicted obesity in an independent population of CC-RIX mice  
333 and in humans, whereas a model using local gene regulation alone was unable to predict obesity in the mice.  
334 Finally, we showed that these transcriptomic signatures have multiple applications, including analyses of  
335 tissue composition from bulk RNA-Seq and drug prioritization.

336 The observation that distal gene regulation is primarily responsible for expression-mediated trait variation  
337 is supported in human studies. Transcripts with low local heritability have been shown to explain more  
338 expression-mediated disease heritability than transcripts with high local heritability<sup>19</sup>. Further, studies  
339 suggest that genes that are near GWAS hits and have obvious functional relevance to a trait tend to have  
340 highly complex regulatory landscapes under strong selection pressures<sup>18</sup>. In contrast, genes with strong local  
341 regulation tend to be depleted of functional annotations and are under looser selection constraints<sup>18</sup>. These  
342 observations and others led Liu et al.<sup>61</sup> to suggest that most heritability of complex traits is driven by weak  
343 distal eQTLs. They proposed a framework of understanding heritability of complex traits in which massive  
344 polygenicity is distributed across common variants in both functional “core genes”, as well as more peripheral  
345 genes that may not seem obviously related to the trait.

346 This pattern is consistent with principles of robustness in complex systems<sup>62–64</sup>. If a transcript were both  
347 important to a trait and subject to strong local regulation, a population would be susceptible to extremes  
348 in phenotype that might frequently cross the threshold to disease. Indeed, strong disruption of highly  
349 trait-relevant genes is the cause of Mendelian disease.

350 Here, we used large, comprehensive, and purpose-built data sets to investigate the genetic architecture of  
351 complex traits related to metabolic disease in mice as well as the roles of local and distal gene regulation  
352 in mediating these traits. We presented a systems-level method called high-dimension mediation analysis  
353 (HDMA) to specifically identify the distally regulated transcriptomic signature mediating the effect of the  
354 genotype on phenotype. This approach contrasts with traditional univariate approaches in several important  
355 respects. First, in contrast to univariate approaches, which assume independence of genetic variants and  
356 transcripts, HDMA allows for arbitrarily complex gene regulation, as well as the interconnectedness and  
357 redundancy of the transcriptome. Second, rather than assuming a single, large genetic effect as univariate  
358 approaches do, HDMA assumes that traits are highly polygenic, and that genetic effects are weak and are  
359 distributed across the genome. HDMA generates a weighted vector of transcripts that can be analyzed  
360 as a whole, or dissected to identify transcripts with stronger and weaker effects. This method explicitly

361 models a central proposal of the omnigenic model which posits that once the expression of the core genes  
362 (i.e. trait-mediating genes) is accounted for, there should be no residual correlation between the genome and  
363 the phenome.

364 Using HDMA, we identified a highly heritable composite trait ( $h^2 = 0.71$ ) that explained 30% of overall trait  
365 variance, and was perfectly mediated by a composite transcript that included expression from four tissues  
366 known to be involved in metabolic disease. Gene expression in adipose tissue was the strongest mediator of  
367 genetic effects on metabolic disease. Further analysis of the loadings onto transcripts in each tissue revealed  
368 that the mediating signatures were tissue-specific transcriptional programs, many of which were previously  
369 known to be involved in the pathogenesis of metabolic disease. We showed here that regulation of these  
370 programs is heritable and mediated a large proportion of disease risk.

371 The transcripts with the highest loadings are similar to the core genes of the omnigenic model [REF]. These  
372 were transcripts of moderate local heritability that were highly functionally related to the traits. Transcripts  
373 with small loadings are more peripheral to the traits measured in this experiment. There was no clear  
374 demarcation between the core and peripheral genes as far as loading, but a clear separation should not be  
375 expected given the complexity of gene regulation and the genotype-phenotype map<sup>65</sup>.

376 The strength of mediation (transcript loading) was negatively correlated with local heritability and positively  
377 correlated with distal heritability, suggesting that distal gene regulation was the dominant mode through which  
378 gene expression mediated the effect of genotype on phenotype. We saw further that the distal heritability  
379 was weak and spread across the genome, consistent with the prediction by Liu *et al.*<sup>61</sup> that trait heritability  
380 is mediated through weak distal eQTLs. Most strongly mediating transcripts had modest distal heritability,  
381 and even for those whose expression was strongly regulated by distal factors, these factors were multiple  
382 and spread across the genome. For example, *Nucb2*, was a strongly mediating transcript in islet and was  
383 also strongly distally regulated (66% distal heritability). This gene is expressed in pancreatic  $\beta$  cells and is  
384 involved in insulin and glucagon release<sup>66–68</sup>. Although its transcription was highly heritable in islets, that  
385 regulation was distributed across the genome, with no clear distal eQTL (Supp. Fig. 5). Thus, although  
386 distal regulation of some genes may be strong, this regulation is likely to be highly complex and not easily  
387 localized.

388 The high complexity of gene regulation combined with a systems-level analysis yields continuous results  
389 that do not necessarily implicate individual transcripts or genetic loci in disease pathogenesis. Most studies  
390 have focused on pinpointing individual loci whose mechanistic roles can be clearly dissected through further  
391 experiments and exploited as therapeutic targets. In this analysis, too, it is possible to focus on individual

392 genes and their context in both tissues and pathways. For example, the loadings on *Pparg* were tissue-specific  
393 in a way that comports with known biology, i.e. it is known to be protective in adipose tissue where it was  
394 negatively loaded, and harmful in the liver, where it was positively loaded. However, whole transcriptomic  
395 signatures can also be informative in their own right. Combined with increasing amounts of high-dimensional  
396 data in public databases, weighted vectors can be useful for generating hypotheses and potential drug  
397 treatments. We showed that weighted vectors of genes can be analyzed for enriched biological functions  
398 and pathways using GSEA. These vectors can also be paired with data about cell-type specific genes to  
399 generate hypotheses about cell composition in individual tissues. Gene expression derived from patient  
400 biopsies confirmed that the transcriptional signatures we identified in mice predict obesity status in humans,  
401 further supporting the translatability of these results. Finally, we used the CMAP database to show that the  
402 transcriptomic signatures we identified in mice could be translated into human drug targets, as currently  
403 used diabetes drugs and targets were among the top hits for reversing the disease-associated signatures. That  
404 these drugs are known to reverse diabetes pathogenesis supports the causal role of these gene signatures in  
405 disease risk as modeled by high-dimensional mediation.

406 In conclusion, we have shown that both tissue specificity and distal gene regulation are critically important to  
407 understanding the genetic architecture of complex traits. We identified important genes and gene signatures  
408 that were heritable, causal of disease, and translatable to other mouse populations and to humans. Finally,  
409 we have shown that by directly acknowledging the complexity of both gene regulation and the genotype-to-  
410 phenotype map, we can gain a new perspective on disease pathogenesis and develop actionable hypotheses  
411 about pathogenic mechanisms and potential treatments.

412 Potentially comment on: 1) Mediating on other endophenotypes 2) Limitation that we only find signatures  
413 “consistent with” mediation and that our approach is hypothesis generating 3) Is the kinship matrix the  
414 sum of all local QTLs, or is it something more inclusive, including distal regulation, development, etc. 4)  
415 endophenotypes don’t need to be gene expression. Can be anything you think is causally related to phenotype  
416 and can be manipulated

## 417 Data Availability

418 Here we tell people where to find the data

## 419 Acknowledgements

420 Here we thank people

421 **Supplemental Figures**

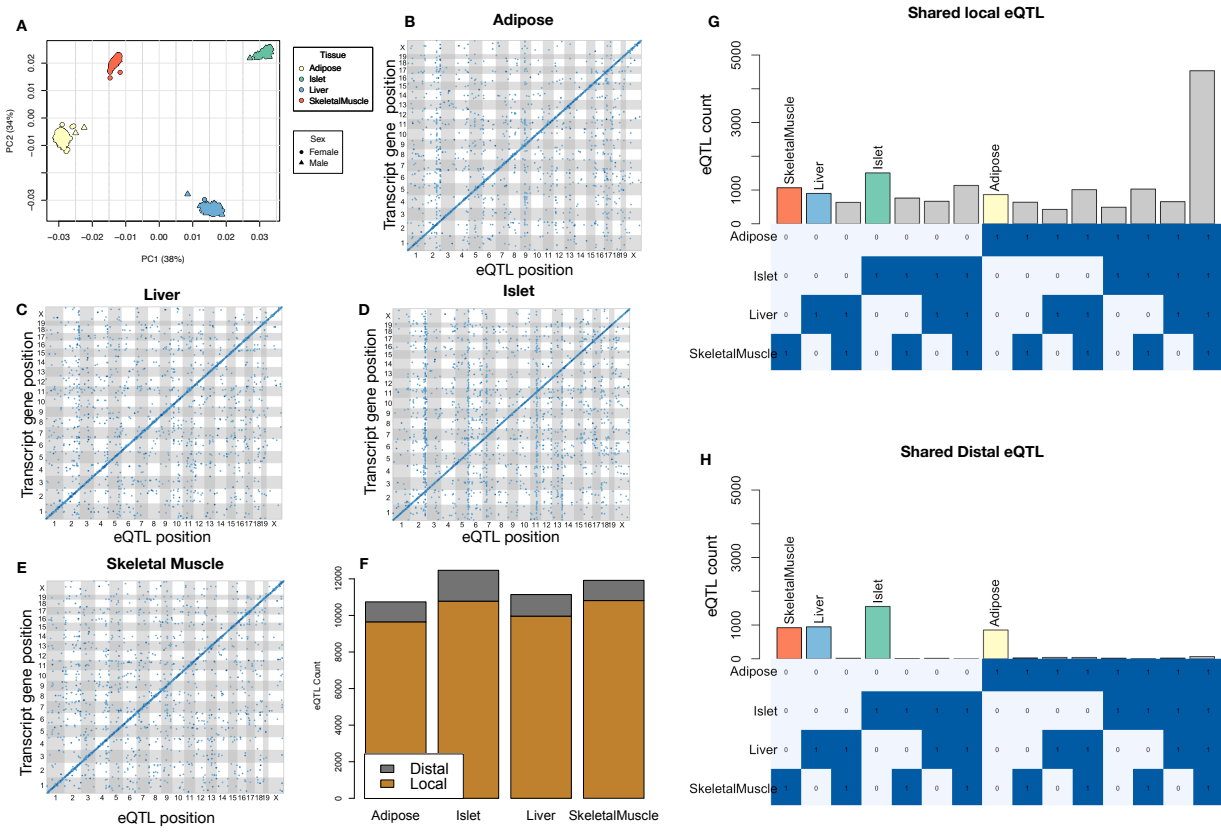


Figure 9: Overview of eQTL analysis in DO mice. **A.** RNA seq samples from the four different tissues clustered by tissue. **B.-E.** eQTL maps are shown for each tissue. The *x*-axis shows the position of the mapped eQTL, and the *y*-axis shows the physical position of the gene encoding each mapped transcript. Each dot represents an eQTL with a minimum LOD score of 8. The dots on the diagonal are locally regulated eQTL for which the mapped eQTL is at the within 4Mb of the encoding gene. Dots off the diagonal are distally regulated eQTL for which the mapped eQTL is distant from the gene encoding the transcript. **F.** Comparison of the total number of local and distal eQTL with a minimum LOD score of 8 in each tissue. All tissues have comparable numbers of eQTL. Local eQTL are much more numerous than distal eQTL. **G.** Counts of transcripts with local eQTL shared across multiple tissues. The majority of local eQTL were shared across all four tissues. **H.** Counts of transcripts with distal eQTL shared across multiple tissues. The majority of distal eQTL were tissue-specific and not shared across multiple tissues. For both G and H, eQTL for a given transcript were considered shared in two tissues if they were within 4Mb of each other. Colored bars indicate the counts for individual tissues for easy of visualization.

422 **References**

- 423 [1] M. T. Maurano, R. Humbert, E. Rynes, R. E. Thurman, E. Haugen, H. Wang, A. P. Reynolds,  
424 R. Sandstrom, H. Qu, J. Brody, A. Shafer, F. Neri, K. Lee, T. Kutyavin, S. Stehling-Sun, A. K.  
425 Johnson, T. K. Canfield, E. Giste, M. Diegel, D. Bates, R. S. Hansen, S. Neph, P. J. Sabo, S. Heimfeld,  
426 A. Raubitschek, S. Ziegler, C. Cotsapas, N. Sotoodehnia, I. Glass, S. R. Sunyaev, R. Kaul, and J. A.

## KEGG pathway enrichments by GSEA

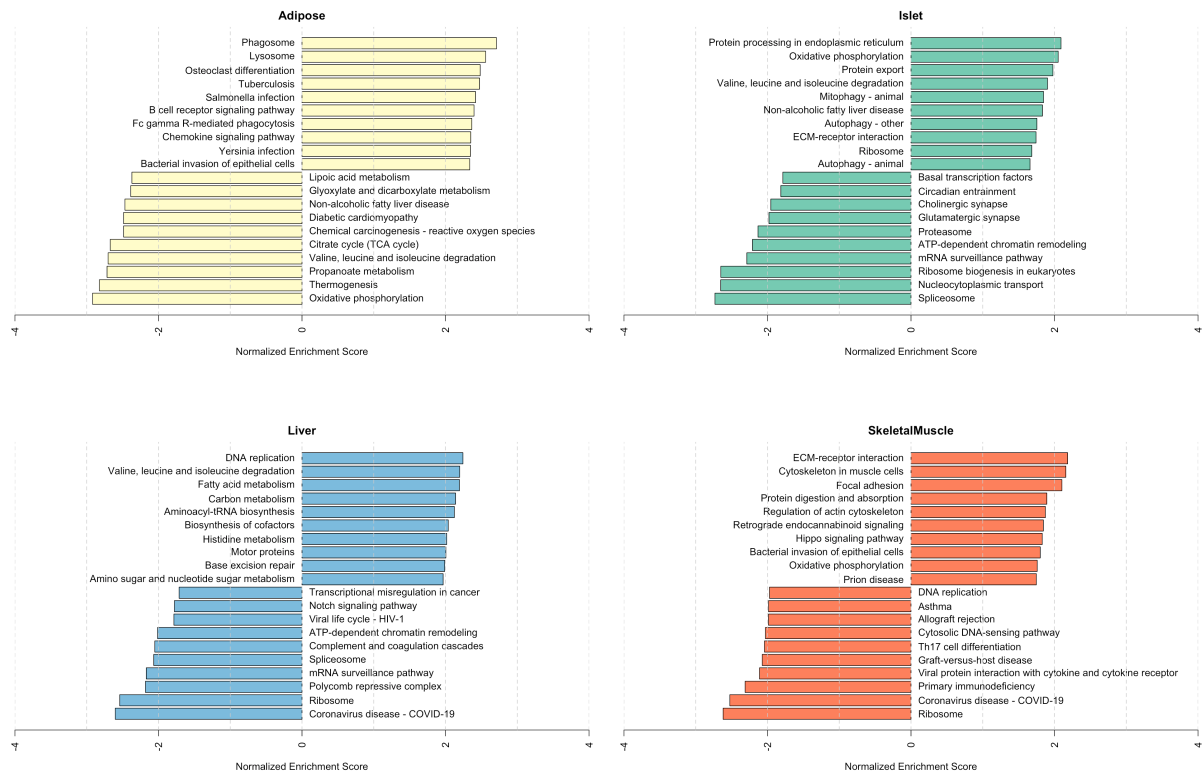


Figure 10: Bar plots showing normalized enrichment scores (NES) for KEGG pathways as determined by fast gene score enrichment analysis (fgsea). Only the top 10 positive and top 10 negative scores are shown. Colors indicate tissue. The name beside each bar shows the name of each enriched KEGG pathway.

- 427 Stamatoyanopoulos. Systematic localization of common disease-associated variation in regulatory DNA.  
 428 *Science*, 337(6099):1190–1195, Sep 2012.
- 429 [2] K. K. Farh, A. Marson, J. Zhu, M. Kleinewietfeld, W. J. Housley, S. Beik, N. Shores, H. Whitton, R. J.  
 430 Ryan, A. A. Shishkin, M. Hatan, M. J. Carrasco-Alfonso, D. Mayer, C. J. Luckey, N. A. Patsopoulos,  
 431 P. L. De Jager, V. K. Kuchroo, C. B. Epstein, M. J. Daly, D. A. Hafler, and B. E. Bernstein. Genetic  
 432 and epigenetic fine mapping of causal autoimmune disease variants. *Nature*, 518(7539):337–343, Feb  
 433 2015.
- 434 [3] E. Pennisi. The Biology of Genomes. Disease risk links to gene regulation. *Science*, 332(6033):1031, May  
 435 2011.
- 436 [4] L. A. Hindorff, P. Sethupathy, H. A. Junkins, E. M. Ramos, J. P. Mehta, F. S. Collins, and T. A. Manolio.

## Top GO term enrichments by GSEA

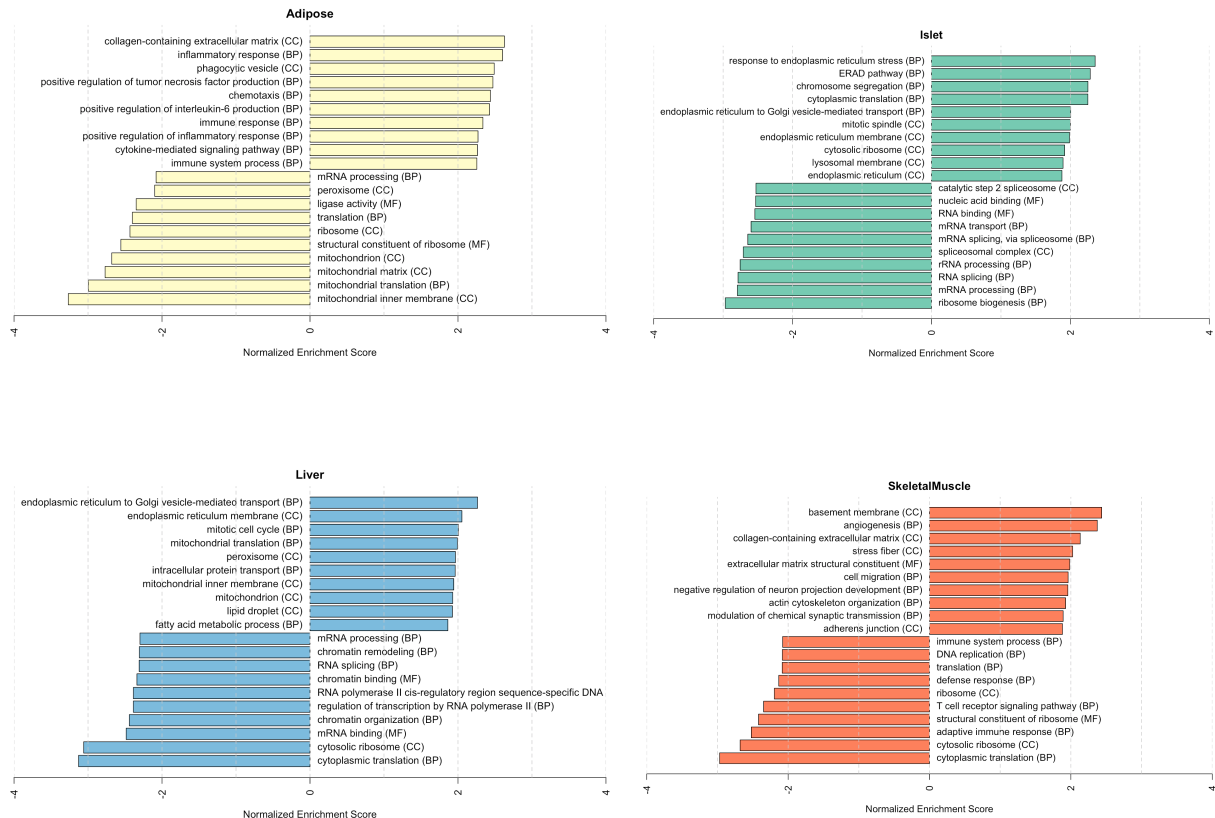


Figure 11: Bar plots showing normalized enrichment scores (NES) for GO terms as determined by fast gene score enrichment analysis (fgsea). Only the top 10 positive and top 10 negative scores are shown. Colors indicate tissue. The name beside each bar shows the name of each enriched GO term. The letters in parentheses indicate whether the term is from the biological process ontology (BP), the molecular function ontology (MF), or the cellular compartment ontology (CC).

437 Potential etiologic and functional implications of genome-wide association loci for human diseases and  
 438 traits. *Proc Natl Acad Sci*, 106(23):9362–9367, Jun 2009.

439 [5] J. K. Pickrell. Joint analysis of functional genomic data and genome-wide association studies of 18  
 440 human traits. *Am J Hum Genet*, 94(4):559–573, Apr 2014.

441 [6] D. Welter, J. MacArthur, J. Morales, T. Burdett, P. Hall, H. Junkins, A. Klemm, P. Flicek, T. Manolio,  
 442 L. Hindorff, and H. Parkinson. The NHGRI GWAS Catalog, a curated resource of SNP-trait associations.  
 443 *Nucleic Acids Res*, 42(Database issue):D1001–1006, Jan 2014.

444 [7] Y. I. Li, B. van de Geijn, A. Raj, D. A. Knowles, A. A. Petti, D. Golan, Y. Gilad, and J. K. Pritchard.  
 445 RNA splicing is a primary link between genetic variation and disease. *Science*, 352(6285):600–604, Apr

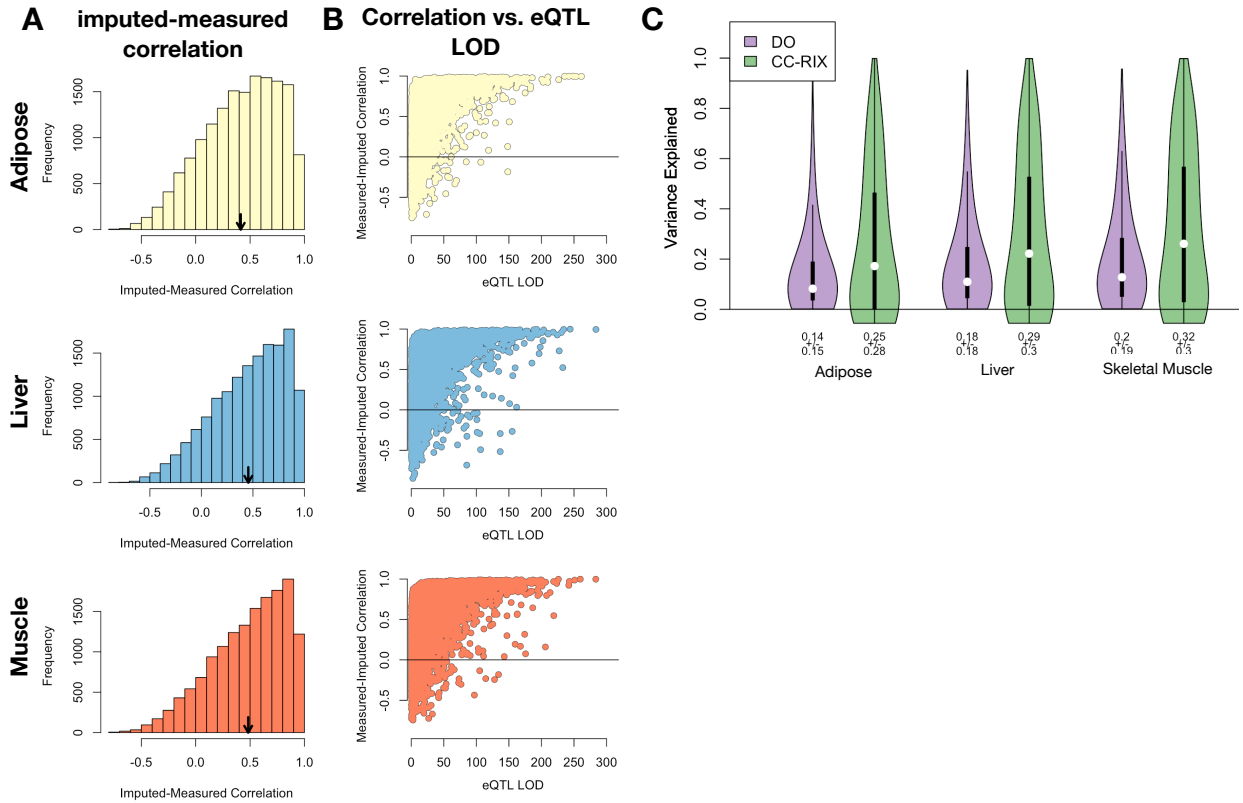


Figure 12: Validation of transcript imputation in the CC-RIX. **A.** Distributions of correlations between imputed and measured transcripts in the CC-RIX. The mean of each distribution is shown by the red line. All distributions were skewed toward positive correlations and had positive means near a Pearson correlation ( $r$ ) of 0.5. **B.** The relationship between the correlation between measured and imputed expression in the CC-RIX (x-axis) and eQTL LOD score. As expected, imputations are more accurate for transcripts with strong local eQTL. **C.** Variance explained by local genotype in the DO and CC-RIX.

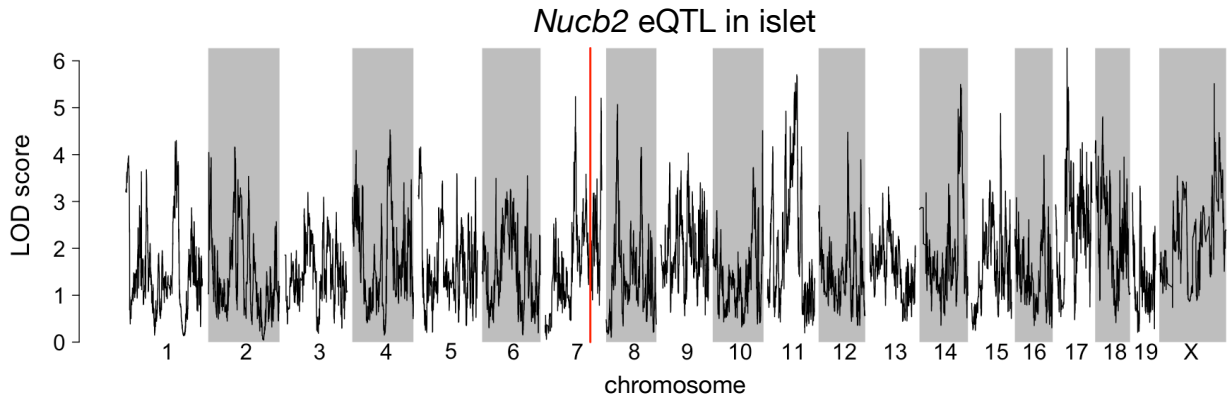


Figure 13: Regulation of *Nucb2* expression in islet. *Nucb2* is encoded on mouse chromosome 7 at 116.5 Mb (red line). In islets the heritability of *Nucb2* expression levels is 69% heritable. This LOD score trace shows that there is no local eQTL at that position, nor any strong distal eQTL anywhere else in the genome.

- 446 2016.
- 447 [8] D. Zhou, Y. Jiang, X. Zhong, N. J. Cox, C. Liu, and E. R. Gamazon. A unified framework for joint-tissue  
448 transcriptome-wide association and Mendelian randomization analysis. *Nat Genet*, 52(11):1239–1246,  
449 Nov 2020.
- 450 [9] E. R. Gamazon, H. E. Wheeler, K. P. Shah, S. V. Mozaffari, K. Aquino-Michaels, R. J. Carroll, A. E.  
451 Eyler, J. C. Denny, D. L. Nicolae, N. J. Cox, and H. K. Im. A gene-based association method for  
452 mapping traits using reference transcriptome data. *Nat Genet*, 47(9):1091–1098, Sep 2015.
- 453 [10] Z. Zhu, F. Zhang, H. Hu, A. Bakshi, M. R. Robinson, J. E. Powell, G. W. Montgomery, M. E. Goddard,  
454 N. R. Wray, P. M. Visscher, and J. Yang. Integration of summary data from GWAS and eQTL studies  
455 predicts complex trait gene targets. *Nat Genet*, 48(5):481–487, May 2016.
- 456 [11] A. Gusev, A. Ko, H. Shi, G. Bhatia, W. Chung, B. W. Penninx, R. Jansen, E. J. de Geus, D. I. Boomsma,  
457 F. A. Wright, P. F. Sullivan, E. Nikkola, M. Alvarez, M. Civelek, A. J. Lusis, T. ki, E. Raitoharju,  
458 M. nen, I. ä, O. T. Raitakari, J. Kuusisto, M. Laakso, A. L. Price, P. Pajukanta, and B. Pasaniuc.  
459 Integrative approaches for large-scale transcriptome-wide association studies. *Nat Genet*, 48(3):245–252,  
460 Mar 2016.
- 461 [12] M. P. Keller, D. M. Gatti, K. L. Schueler, M. E. Rabaglia, D. S. Stapleton, P. Simecek, M. Vincent,  
462 S. Allen, A. T. Broman, R. Bacher, C. Kendziorski, K. W. Broman, B. S. Yandell, G. A. Churchill, and  
463 A. D. Attie. Genetic Drivers of Pancreatic Islet Function. *Genetics*, 209(1):335–356, May 2018.
- 464 [13] W. L. Crouse, G. R. Keele, M. S. Gastonguay, G. A. Churchill, and W. Valdar. A Bayesian model  
465 selection approach to mediation analysis. *PLoS Genet*, 18(5):e1010184, May 2022.
- 466 [14] J. M. Chick, S. C. Munger, P. Simecek, E. L. Huttlin, K. Choi, D. M. Gatti, N. Raghupathy, K. L. Svenson,  
467 G. A. Churchill, and S. P. Gygi. Defining the consequences of genetic variation on a proteome-wide scale.  
468 *Nature*, 534(7608):500–505, Jun 2016.
- 469 [15] H. E. Wheeler, S. Ploch, A. N. Barbeira, R. Bonazzola, A. Andaleon, A. Fotuhi Siahpirani, A. Saha,  
470 A. Battle, S. Roy, and H. K. Im. Imputed gene associations identify replicable trans-acting genes enriched  
471 in transcription pathways and complex traits. *Genet Epidemiol*, 43(6):596–608, Sep 2019.
- 472 [16] B. D. Umans, A. Battle, and Y. Gilad. Where Are the Disease-Associated eQTLs? *Trends Genet*,  
473 37(2):109–124, Feb 2021.
- 474 [17] N. J. Connally, S. Nazeen, D. Lee, H. Shi, J. Stamatoyannopoulos, S. Chun, C. Cotsapas, C. A. Cassa,

- 475 and S. R. Sunyaev. The missing link between genetic association and regulatory function. *Elife*, 11, Dec  
476 2022.
- 477 [18] H. Mostafavi, J. P. Spence, S. Naqvi, and J. K. Pritchard. Systematic differences in discovery of genetic  
478 effects on gene expression and complex traits. *Nat Genet*, 55(11):1866–1875, Nov 2023.
- 479 [19] D. W. Yao, L. J. O’Connor, A. L. Price, and A. Gusev. Quantifying genetic effects on disease mediated  
480 by assayed gene expression levels. *Nat Genet*, 52(6):626–633, Jun 2020.
- 481 [20] X. Liu, J. A. Mefford, A. Dahl, Y. He, M. Subramaniam, A. Battle, A. L. Price, and N. Zaitlen. GBAT:  
482 a gene-based association test for robust detection of trans-gene regulation. *Genome Biol*, 21(1):211, Aug  
483 2020.
- 484 [21] G. A. Churchill, D. M. Gatti, S. C. Munger, and K. L. Svenson. The Diversity Outbred mouse population.  
485 *Mamm Genome*, 23(9-10):713–718, Oct 2012.
- 486 [22] Michael C Saul, Vivek M Philip, Laura G Reinholdt, and Elissa J Chesler. High-diversity mouse  
487 populations for complex traits. *Trends in Genetics*, 35(7):501–514, 2019.
- 488 [23] S. M. Clee and A. D. Attie. The genetic landscape of type 2 diabetes in mice. *Endocr Rev*, 28(1):48–83,  
489 Feb 2007.
- 490 [24] K. W. Broman, D. M. Gatti, P. Simecek, N. A. Furlotte, P. Prins, Š. Sen, B. S. Yandell, and G. A.  
491 Churchill. R/qt12: Software for Mapping Quantitative Trait Loci with High-Dimensional Data and  
492 Multiparent Populations. *Genetics*, 211(2):495–502, Feb 2019.
- 493 [25] Fabien Girka, Etienne Camenen, Caroline Peltier, Arnaud Gloaguen, Vincent Guillemot, Laurent Le  
494 Brusquet, and Arthur Tenenhaus. *RGCCA: Regularized and Sparse Generalized Canonical Correlation*  
495 *Analysis for Multiblock Data*, 2023. R package version 3.0.3.
- 496 [26] Gennady Korotkevich, Vladimir Sukhov, and Alexey Sergushichev. Fast gene set enrichment analysis.  
497 *bioRxiv*, 2019.
- 498 [27] A. Subramanian, P. Tamayo, V. K. Mootha, S. Mukherjee, B. L. Ebert, M. A. Gillette, A. Paulovich,  
499 S. L. Pomeroy, T. R. Golub, E. S. Lander, and J. P. Mesirov. Gene set enrichment analysis: a  
500 knowledge-based approach for interpreting genome-wide expression profiles. *Proc Natl Acad Sci U S A*,  
501 102(43):15545–15550, Oct 2005.
- 502 [28] C. B. Newgard. Interplay between lipids and branched-chain amino acids in development of insulin  
503 resistance. *Cell Metab*, 15(5):606–614, May 2012.

- 504 [29] D. D. Sears, G. Hsiao, A. Hsiao, J. G. Yu, C. H. Courtney, J. M. Ofrecio, J. Chapman, and S. Subramaniam.  
505 Mechanisms of human insulin resistance and thiazolidinedione-mediated insulin sensitization. *Proc Natl  
506 Acad Sci U S A*, 106(44):18745–18750, Nov 2009.
- 507 [30] R. Stienstra, C. Duval, M. ller, and S. Kersten. PPARs, Obesity, and Inflammation. *PPAR Res*,  
508 2007:95974, 2007.
- 509 [31] O. Gavrilova, M. Haluzik, K. Matsusue, J. J. Cutson, L. Johnson, K. R. Dietz, C. J. Nicol, C. Vinson,  
510 F. J. Gonzalez, and M. L. Reitman. Liver peroxisome proliferator-activated receptor gamma contributes  
511 to hepatic steatosis, triglyceride clearance, and regulation of body fat mass. *J Biol Chem*, 278(36):34268–  
512 34276, Sep 2003.
- 513 [32] K. Matsusue, M. Haluzik, G. Lambert, S. H. Yim, O. Gavrilova, J. M. Ward, B. Brewer, M. L. Reitman,  
514 and F. J. Gonzalez. Liver-specific disruption of PPARgamma in leptin-deficient mice improves fatty  
515 liver but aggravates diabetic phenotypes. *J Clin Invest*, 111(5):737–747, Mar 2003.
- 516 [33] D. Patsouris, J. K. Reddy, M. ller, and S. Kersten. Peroxisome proliferator-activated receptor alpha  
517 mediates the effects of high-fat diet on hepatic gene expression. *Endocrinology*, 147(3):1508–1516, Mar  
518 2006.
- 519 [34] S. E. Schadinger, N. L. Bucher, B. M. Schreiber, and S. R. Farmer. PPARgamma2 regulates lipogenesis  
520 and lipid accumulation in steatotic hepatocytes. *Am J Physiol Endocrinol Metab*, 288(6):E1195–1205,  
521 Jun 2005.
- 522 [35] W. Motomura, M. Inoue, T. Ohtake, N. Takahashi, M. Nagamine, S. Tanno, Y. Kohgo, and T. Okumura.  
523 Up-regulation of ADRP in fatty liver in human and liver steatosis in mice fed with high fat diet. *Biochem  
524 Biophys Res Commun*, 340(4):1111–1118, Feb 2006.
- 525 [36] S. Amin, A. Lux, and F. O’Callaghan. The journey of metformin from glycaemic control to mTOR  
526 inhibition and the suppression of tumour growth. *Br J Clin Pharmacol*, 85(1):37–46, Jan 2019.
- 527 [37] A. Kezic, L. Popovic, and K. Lalic. mTOR Inhibitor Therapy and Metabolic Consequences: Where Do  
528 We Stand? *Oxid Med Cell Longev*, 2018:2640342, 2018.
- 529 [38] A. D. Barlow, M. L. Nicholson, and T. P. Herbert. -cells and a review of the underlying molecular  
530 mechanisms. *Diabetes*, 62(8):2674–2682, Aug 2013.
- 531 [39] Y. Gu, J. Lindner, A. Kumar, W. Yuan, and M. A. Magnuson. Rictor/mTORC2 is essential for  
532 maintaining a balance between beta-cell proliferation and cell size. *Diabetes*, 60(3):827–837, Mar 2011.

- 533 [40] E. B. Geer, J. Islam, and C. Buettner. Mechanisms of glucocorticoid-induced insulin resistance: focus on  
534 adipose tissue function and lipid metabolism. *Endocrinol Metab Clin North Am*, 43(1):75–102, Mar 2014.
- 535 [41] J. X. Li and C. L. Cummins. Fresh insights into glucocorticoid-induced diabetes mellitus and new  
536 therapeutic directions. *Nat Rev Endocrinol*, 18(9):540–557, Sep 2022.
- 537 [42] R. A. Lee, C. A. Harris, and J. C. Wang. Glucocorticoid Receptor and Adipocyte Biology. *Nucl Receptor  
538 Res*, 5, 2018.
- 539 [43] S. Viengchareun, P. Penfornis, M. C. Zennaro, and M. s. Mineralocorticoid and glucocorticoid receptors  
540 inhibit UCP expression and function in brown adipocytes. *Am J Physiol Endocrinol Metab*, 280(4):E640–  
541 649, Apr 2001.
- 542 [44] J. Liu, X. Kong, L. Wang, H. Qi, W. Di, X. Zhang, L. Wu, X. Chen, J. Yu, J. Zha, S. Lv, A. Zhang,  
543 P. Cheng, M. Hu, Y. Li, J. Bi, Y. Li, F. Hu, Y. Zhong, Y. Xu, and G. Ding. -HSD1 in regulating brown  
544 adipocyte function. *J Mol Endocrinol*, 50(1):103–113, Feb 2013.
- 545 [45] L. E. Ramage, M. Akyol, A. M. Fletcher, J. Forsythe, M. Nixon, R. N. Carter, E. J. van Beek,  
546 N. M. Morton, B. R. Walker, and R. H. Stimson. Glucocorticoids Acutely Increase Brown Adipose  
547 Tissue Activity in Humans, Revealing Species-Specific Differences in UCP-1 Regulation. *Cell Metab*,  
548 24(1):130–141, Jul 2016.
- 549 [46] J. L. Barclay, H. Agada, C. Jang, M. Ward, N. Wetzig, and K. K. Ho. Effects of glucocorticoids on  
550 human brown adipocytes. *J Endocrinol*, 224(2):139–147, Feb 2015.
- 551 [47] M. ó, R. Gupte, W. L. Kraus, P. Pacher, and P. Bai. PARPs in lipid metabolism and related diseases.  
552 *Prog Lipid Res*, 84:101117, Nov 2021.
- 553 [48] P. Bai, C. ó, H. Oudart, A. nszki, Y. Cen, C. Thomas, H. Yamamoto, A. Huber, B. Kiss, R. H.  
554 Houtkooper, K. Schoonjans, V. Schreiber, A. A. Sauve, J. Menissier-de Murcia, and J. Auwerx. PARP-1  
555 inhibition increases mitochondrial metabolism through SIRT1 activation. *Cell Metab*, 13(4):461–468,  
556 Apr 2011.
- 557 [49] A. Chiarugi and M. A. Moskowitz. Cell biology. PARP-1—a perpetrator of apoptotic cell death? *Science*,  
558 297(5579):200–201, Jul 2002.
- 559 [50] M. Althubiti, R. Almaimani, S. Y. Eid, M. Elzubaier, B. Refaat, S. Idris, T. A. Alqurashi, and M. Z.  
560 El-Readi. BTK targeting suppresses inflammatory genes and ameliorates insulin resistance. *Eur Cytokine  
561 Netw*, 31(4):168–179, Dec 2020.

- 562 [51] C. Skrabs, W. F. Pickl, T. Perkmann, U. ger, and A. Gessl. Rapid decline in insulin antibodies and  
563 glutamic acid decarboxylase autoantibodies with ibrutinib therapy of chronic lymphocytic leukaemia. *J*  
564 *Clin Pharm Ther*, 43(1):145–149, Feb 2018.
- 565 [52] E. A. Oral, S. M. Reilly, A. V. Gomez, R. Meral, L. Butz, N. Ajluni, T. L. Chenevert, E. Korytnaya,  
566 A. H. Neidert, R. Hench, D. Rus, J. F. Horowitz, B. Poirier, P. Zhao, K. Lehmann, M. Jain, R. Yu,  
567 C. Liddle, M. Ahmadian, M. Downes, R. M. Evans, and A. R. Saltiel. and TBK1 Improves Glucose  
568 Control in a Subset of Patients with Type 2 Diabetes. *Cell Metab*, 26(1):157–170, Jul 2017.
- 569 [53] M. C. Arkan, A. L. Hevener, F. R. Greten, S. Maeda, Z. W. Li, J. M. Long, A. Wynshaw-Boris, G. Poli,  
570 J. Olefsky, and M. Karin. IKK-beta links inflammation to obesity-induced insulin resistance. *Nat Med*,  
571 11(2):191–198, Feb 2005.
- 572 [54] M. Clark, C. J. Kroger, Q. Ke, and R. M. Tisch. The Role of T Cell Receptor Signaling in the  
573 Development of Type 1 Diabetes. *Front Immunol*, 11:615371, 2020.
- 574 [55] P. ndell, A. C. Carlsson, A. Larsson, O. Melander, T. Wessman, J. v, and T. Ruge. TNFR1 is associated  
575 with short-term mortality in patients with diabetes and acute dyspnea seeking care at the emergency  
576 department. *Acta Diabetol*, 57(10):1145–1150, Oct 2020.
- 577 [56] A. M. Keestra-Gounder, M. X. Byndloss, N. Seyffert, B. M. Young, A. vez Arroyo, A. Y. Tsai, S. A.  
578 Cevallos, M. G. Winter, O. H. Pham, C. R. Tiffany, M. F. de Jong, T. Kerrinnes, R. Ravindran, P. A.  
579 Luciw, S. J. McSorley, A. J. umler, and R. M. Tsolis. NOD1 and NOD2 signalling links ER stress with  
580 inflammation. *Nature*, 532(7599):394–397, Apr 2016.
- 581 [57] A. M. Keestra-Gounder and R. M. Tsolis. NOD1 and NOD2: Beyond Peptidoglycan Sensing. *Trends*  
582 *Immunol*, 38(10):758–767, Oct 2017.
- 583 [58] J. Montane, L. Cadavez, and A. Novials. Stress and the inflammatory process: a major cause of  
584 pancreatic cell death in type 2 diabetes. *Diabetes Metab Syndr Obes*, 7:25–34, 2014.
- 585 [59] B. B. Kahn and T. E. McGraw. , and type 2 diabetes. *N Engl J Med*, 363(27):2667–2669, Dec 2010.
- 586 [60] S. Del Prato and N. Pulizzi. The place of sulfonylureas in the therapy for type 2 diabetes mellitus.  
587 *Metabolism*, 55(5 Suppl 1):S20–27, May 2006.
- 588 [61] X. Liu, Y. I. Li, and J. K. Pritchard. Trans Effects on Gene Expression Can Drive Omnipotent Inheritance.  
589 *Cell*, 177(4):1022–1034, May 2019.
- 590 [62] B. Hallgrímsson, R. M. Green, D. C. Katz, J. L. Fish, F. P. Bernier, C. C. Roseman, N. M. Young,

- 591 J. M. Cheverud, and R. S. Marcucio. The developmental-genetics of canalization. *Semin Cell Dev Biol*,  
592 88:67–79, Apr 2019.
- 593 [63] M. L. Siegal and A. Bergman. Waddington’s canalization revisited: developmental stability and evolution.  
594 *Proc Natl Acad Sci U S A*, 99(16):10528–10532, Aug 2002.
- 595 [64] A. B. Paaby and G. Gibson. Cryptic Genetic Variation in Evolutionary Developmental Genetics. *Biology*  
596 (*Basel*), 5(2), Jun 2016.
- 597 [65] Naomi R Wray, Cisca Wijmenga, Patrick F Sullivan, Jian Yang, and Peter M Visscher. Common disease  
598 is more complex than implied by the core gene omnigenic model. *Cell*, 173(7):1573–1580, 2018.
- 599 [66] M. Riva, M. D. Nitert, U. Voss, R. Sathanoori, A. Lindqvist, C. Ling, and N. Wierup. Nesfatin-1  
600 stimulates glucagon and insulin secretion and beta cell NUCB2 is reduced in human type 2 diabetic  
601 subjects. *Cell Tissue Res*, 346(3):393–405, Dec 2011.
- 602 [67] M. Nakata and T. Yada. Role of NUCB2/nesfatin-1 in glucose control: diverse functions in islets,  
603 adipocytes and brain. *Curr Pharm Des*, 19(39):6960–6965, 2013.
- 604 [68] H. Shimizu and A. Osaki. Nesfatin/Nucleobindin-2 (NUCB2) and Glucose Homeostasis. *Curr Hypertens*  
605 *Rev*, pages Nesfatin/Nucleobindin–2 (NUCB2) and Glucose Homeostasis., Jul 2014.